

AD-A058 396

AIR FORCE INST OF TECH WRIGHT-PATTERSON AFB OHIO
AN ANALYSIS OF THE RELATIONSHIP BETWEEN SULFUR DIOXIDE AND WIND--ETC(U)

F/G 13/2

MAR 78 M G COLEMAN
AFIT-CI-78-60

NL

UNCLASSIFIED

1 OF 1
AD
A058 396



END
DATE
FILMED
-11-78
DDC

UNCLASSIFIED

SECURITY CLASSIFICATION OF THIS PAGE (When Data Entered)

REPORT DOCUMENTATION PAGE

READ INSTRUCTIONS BEFORE COMPLETING FORM

1. REPORT NUMBER

2. GOVT ACCESSION NO.

3. RECIPIENT'S CATALOG NUMBER

14 AFIT-CI-78-60

4. TITLE (and Subtitle)

An Analysis of the Relationship Between Sulfur Dioxide and Wind Speed,

5. TYPE OF REPORT & PERIOD COVERED
9 Master's Thesis

7. AUTHOR(s)

10 Captain Marvin Granville/Coleman

LEVEL II

9. PERFORMING ORGANIZATION NAME AND ADDRESS

AFIT Student at the University of Utah, Salt Lake City UT

10. PROGRAM ELEMENT, PROJECT, TASK AREA & WORK UNIT NUMBERS

11. CONTROLLING OFFICE NAME AND ADDRESS

AFIT/CI
WPAFB OH 45433

11 Mar 1978

12. REPORT DATE

13. NUMBER OF PAGES

72 Pages 1285p.

14. MONITORING AGENCY NAME & ADDRESS (if different from Controlling Office)

15. SECURITY CLASS. (of this report)

Unclassified

15a. DECLASSIFICATION/DOWNGRADING SCHEDULE

16. DISTRIBUTION STATEMENT (of this Report)

Approved for Public Release; Distribution Unlimited

17. DISTRIBUTION STATEMENT (of the abstract entered in Block 20, if different from Report)

DDC
RECEIVED
SEP 11 1978
F

18. SUPPLEMENTARY NOTES

JOSEPH P. HIPPS, Major, USAF
Director of Information, AFIT

AUG 15 1978

19. KEY WORDS (Continue on reverse side if necessary and identify by block number)

20. ABSTRACT (Continue on reverse side if necessary and identify by block number)

012 200 3
78 08 31 015
Jmac

ADA 058396

DDC FILE COPY

AN ANALYSIS OF THE RELATIONSHIP BETWEEN
SULFUR DIOXIDE AND WIND SPEED

by

Marvin Granville Coleman

A thesis submitted to the faculty of The
University of Utah in partial fulfillment of the requirements
for the degree of

Master of Science

~~Department of Meteorology~~

The University of Utah

March 1978

78-607

The following is submitted IAW AFITR 53-1, para. 7-2:

- a. Author: MARVIN GRANVILLE COLEMAN
- b. Title: AN ANALYSIS OF THE RELATIONSHIP BETWEEN
SULFUR DIOXIDE AND WIND SPEED
- c. Rank/Service: Captain, USAF
- d. Date: 1978
- e. Pages: 73
- f. Degree Awarded: Master of Science
- g. Institution: University of Utah

ACCESSION for	
NTIS	White Section <input checked="" type="checkbox"/>
DDC	Buff Section <input type="checkbox"/>
UNANNOUNCED JUSTIFICATION	
BY DISTRIBUTION/AVAILABILITY CODES	
Dist.	1. ALL. 2. NO. or SPECIAL
A	

AN ANALYSIS OF THE RELATIONSHIP BETWEEN
SULFUR DIOXIDE AND WIND SPEED

by

Marvin Granville Coleman

An abstract of a thesis submitted to the faculty of The
University of Utah in partial fulfillment of the requirements
for the degree of

Master of Science

Shih-Kung Kao

Chairman, Supervisory Committee

Department of Meteorology

Department of Meteorology

The University of Utah

March 1978

78-08 31 015

THE UNIVERSITY OF UTAH GRADUATE SCHOOL

SUPERVISORY COMMITTEE APPROVAL

of a thesis submitted by

Marvin Granville Coleman

I have read this thesis and have found it to be of satisfactory quality for a master's degree.

Feb. 22, 1978

Date

S. K. Kao

S. K. Kao

Chairman, Supervisory Committee

I have read this thesis and have found it to be of satisfactory quality for a master's degree.

Feb. 21, 1978

Date

Kuo-Nan Liou

Kuo-Nan Liou

Member, Supervisory Committee

I have read this thesis and have found it to be of satisfactory quality for a master's degree.

Feb. 21, 1978

Date

Elford G. Astling

Elford G. Astling

Member, Supervisory Committee

THE UNIVERSITY OF UTAH GRADUATE SCHOOL

FINAL READING APPROVAL

To the Graduate Council of The University of Utah:

I have read the thesis of Marvin Granville Coleman in its final form and have found that (1) its format, citations, and bibliographic style are consistent and acceptable; (2) its illustrative materials including figures, tables, and charts are in place; and (3) the final manuscript is satisfactory to the Supervisory Committee and is ready for submission to the Graduate School.

Feb. 22, 1978
Date

S. K. Kao
S. K. Kao
Member, Supervisory Committee

Approved for the Major Department

S. K. Kao

S. K. Kao
Chairman, Dean

Approved for the Graduate Council

Sterling M. McMurrin
Dean of The Graduate School

ABSTRACT

A study of turbulent diffusion in the surface boundary layer is conducted to determine the effects of the wind speed on the distribution of sulfur dioxide (SO_2) with time. With the use of auto-correlograms and the spectra of wind speed and SO_2 , similarities between these scalar quantities under varying stability conditions are investigated. Pollution monitoring sites in the Salt Lake Valley vicinity and St. Louis are used.

Under stable conditions, the auto-correlograms and the spectra of wind speed and SO_2 are similar in many respects. The auto-correlograms show very similar coefficients up to a time lag of 13 hours, and the spectra shows similar peaks near periods of 24, 12 and 8 hours. The wind speed peaks are more prominent, which suggests the spectrum of SO_2 is affected by the spectrum of the wind speed for periods equal to or less than 24 hours. Forecasting the SO_2 spectrum from the wind speed spectrum is possible for the periods near 24 and 12 hours.

The similarity between the wind speed and SO_2 auto-correlograms and spectra decreases as stability decreases. In the stable periods, the effect of the large scale motions is suppressed, and more energy is found in the higher frequencies than in neutral or unstable periods.

ACKNOWLEDGMENTS

My most sincere appreciation and gratitude are extended to Dr. Shih-Kung Kao for his valuable instruction and guidance. Also, my thanks to other members of my supervisory committee, Dr. Elford G. Astling and Dr. Kuo-Nan Liou.

Mr. Robert Dalley of the Utah State Division of Health, Bureau of Environmental Health - Air Quality Section deserves thanks for providing the data from the Salt Lake vicinity stations.

Finally, thanks to my wife, Catherine, for her understanding and assistance throughout the many hours of research.

TABLE OF CONTENTS

	Page
ABSTRACT	iv
ACKNOWLEDGMENTS.	v
LIST OF FIGURES.	viii
Chapter	
1. INTRODUCTION	1
2. APPLICABLE STATISTICAL THEORY.	3
3. METHODS OF CALCULATION	8
R_{VE} and R_{CE}	8
The Spectrum	10
4. DATA	13
Salt Lake City Vicinity.	13
St. Louis.	13
Monitoring Equipment	16
Averaging.	17
5. STABILITY CATEGORY DETERMINATION	19
Stability Indices.	19
Quantity of Data	22
Degrees of Freedom	23
6. RESULTS AND CONCLUSIONS.	25
Auto-correlograms.	25
Cross-correlograms	32
Comparison of SO ₂ and Wind Speed Spectrum.	32
The Inertial Sub-range	43
Lake/River Effects	47
Effects of Local Wind Patterns on the Spectra.	50
7. SUMMARY.	58
APPENDIX A - AUTO- AND CROSSCORRELATION PROGRAMS	60

	Page
APPENDIX B - SPECTRAL DENSITY PROGRAMS	65
REFERENCES	72
VITA	73

LIST OF FIGURES

Figure	Page
1. Auto-correlogram of the wind speed at Magna under neutral conditions	9
2. Base map of the Salt Lake Valley and Vicinity.	14
3. Base map of St. Louis.	15
4. Auto-correlogram of Magna under stable conditions using a 24 hour moving average	26
5. Auto-correlogram of Magna under neutral conditions using a 24 hour moving average	27
6. Auto-correlogram of Magna under unstable conditions using a 24 hour moving average	29
7. Auto-correlogram of Magna using a 24 hour moving average with wind speed (top) and SO ₂ (bottom)	30
8. Auto-correlogram of Magna after eliminating the linear trend with wind speed (top) and SO ₂ (bottom)	31
9. Cross-correlogram of Magna vs. Kearns under stable conditions	33
10. Normalized spectral density of Magna under stable conditions with wind speed (top) and SO ₂ (bottom).	35
11. Normalized spectral density of Magna under neutral conditions with wind speed (top) and SO ₂ (bottom).	37
12. Normalized spectral density of Magna under unstable conditions with wind speed (top) and SO ₂ (bottom).	38
13. Normalized spectral density of the wind speed for urban St. Louis under stable conditions (top) and neutral (bottom)	39
14. Normalized spectral density of the SO ₂ for urban St. Louis under stable conditions (top) and neutral (bottom)	40

Figure	Page
15. Normalized spectral density of the wind speed for suburban St. Louis under stable conditions (top) and neutral (bottom)	41
16. Normalized spectral density of the SO ₂ for suburban St. Louis under stable conditions (top) and neutral (bottom)	42
17. Normalized spectral density of the wind speed at Magna under stable conditions (top), neutral (middle) and unstable (bottom)	48
18. Normalized spectral density of the SO ₂ at Magna under stable conditions (top), neutral (middle) and unstable (bottom).	49
19. Normal spectral density of the SO ₂ at Kearns under stable conditions.	51
20. Normalized spectral density of the SO ₂ at Tooele under stable conditions.	52
21. Normalized spectral density of the wind speed at Bountiful under stable conditions (top) and neutral (bottom)	53
22. Normalized spectral density of the SO ₂ at Bountiful under stable conditions (top) and neutral (bottom)	54
23. Wind rose of Bountiful under stable conditions (top) and neutral (bottom)	56
24. Wind rose of Magna under stable conditions (top) and neutral (bottom)	57

Chapter 1

INTRODUCTION

In the study of boundary layer diffusion with application to air pollution concentration forecasting, many forecast models have been developed. The most important variables in most of the models are the mean wind at varying levels through the boundary layer and diffusion parameters such as turbulence intensity and thermal stratification.

It is known that the power spectrum of wind which is a vector quantity is not necessarily similar to that of pollution concentration which is a scalar quantity. However, since diffusion is a consequence of turbulent motion, the power spectrum of turbulent wind speed which is a scalar quantity may bear some similarity to that of pollution concentration. Should such a similarity be established, portions of the pollution concentration spectrum can be predicted by the spectrum of wind speed. The purpose of this study is to test such an hypothesis.

The autocorrelation coefficients and the spectra for wind speed and SO_2 were calculated for air pollution monitoring sites in the Salt Lake City vicinity and from urban and suburban sites in the St. Louis area. Salt Lake City and St. Louis were chosen for their different physical environments and amount of data.

This paper consists of five major sections. The first

section deals with statistical theory which is applicable to calculating diffusion parameters. The second section deals with the methods used in this paper for calculating the autocorrelation coefficients and spectra. The third section describes the topography of the Salt Lake vicinity and St. Louis, and the type and location of monitoring sites. The fourth section contains a discussion of how the stability categories were determined and the quantity of data available. In section five, the results and conclusions of this study are presented. Finally, a quick summary of the conclusions is in the last section.

Chapter 2

APPLICABLE STATISTICAL THEORY

In the study of atmospheric diffusion two basic theories exist: the K or gradient transport theory, and the statistical theory. The K-theory is derived in Eulerian space. The values of eddy diffusivities derived from K-theory appear in the Gaussian continuous point source equation (1) and are a function of space. The statistical theory is derived in Lagrangian space and the corresponding Gaussian continuous point source equation is (2) in which $\sigma_y(t)$ and $\sigma_z(t)$ are a function of time. Other models also employ the use of Lagrangian diffusion parameters (σ).

$$\bar{C}(x,y,z) = \frac{Q}{4\pi\bar{u}K_{yy}K_{zz}} \exp - \left[\frac{y^2}{4K_{yy}} + \frac{z^2}{4K_{zz}} \right] \quad (1)$$

$$\bar{C}(x,y,z) = \frac{Q}{2\pi\bar{u}\sigma_y(t)\sigma_z(t)} \exp - \left[\frac{y^2}{2\sigma_y^2(t)} + \frac{z^2}{2\sigma_z^2(t)} \right] \quad (2)$$

$\bar{C}(x,y,z)$ is the average concentration at the desired point, \bar{u} is the mean wind velocity, and Q is the rate of emission of effluent.

The values of K_{yy} and K_{zz} are related to $\sigma_y^2(t)$ and $\sigma_z^2(t)$. As $t \rightarrow \infty$ $\sigma_y^2(t) \rightarrow 2K_{yy}t$ and $\sigma_z^2(t) \rightarrow 2K_{zz}t$. Thus, K-theory is a special case of the statistical theory. But in mesoscale diffusion, such as the Salt Lake Valley and St. Louis metropolitan area, t is of the order of hours. Therefore, statistical theory is more accurate for

these areas.

Equation (2) is used when calculating pollution concentration downwind of a point source which is emitting effluent at a steady continuous rate over flat terrain. The most important terms in the equation, or any pollution model equations, are the \bar{u} and the diffusion parameters. \bar{u} must be steady and uni-directional and $\sigma_y(t)$ and $\sigma_z(t)$ are a function of atmospheric turbulence, space and time. This work is aimed at a better understanding of the diffusion parameters ($\sigma_y^2(t)$ and $\sigma_z^2(t)$) and how they vary with atmospheric stability.

In order to apply the Gaussian equation to predict concentration, $\sigma_y^2(t)$ and $\sigma_z^2(t)$ must be known. G. I. Taylor (1921) found the following relationship:

$$\sigma_y^2(t) = 2 \int_0^t \int_0^\eta \langle v_L'(t)v_L'(t') \rangle dt' d\eta \quad (3)$$

where v_L is the Lagrangian turbulent velocity, η is a dummy variable and $\langle v'(t)v'(t') \rangle$ is the autocorrelation function, which may be calculated as an ensemble average of many data samples called realizations.

If v_L' is plotted as the ordinant and t as the abscissa for all realizations then

$$\frac{1}{N} \sum_{j=1}^N [v_{L_j}'(t)v_{L_j}'(t')] = \langle v_L'(t)v_L'(t') \rangle \quad (4)$$

where N is the number of realizations or trails. If the turbulence is homogeneous and stationary, (4) can be written as $\langle v_L'(t)v_L'(t+\tau) \rangle$ where τ is the time lag defined as

$$\tau \equiv t' - t \quad (5)$$

Now (4) is a function of τ not t . The autocorrelation coefficient may then be defined as

$$R_{v_L} = \frac{\langle v_L'(t)v_L'(t+\tau) \rangle}{\langle v_L'^2(t) \rangle} = \frac{\overline{v_L'(t)v_L'(t+\tau)}}{\overline{v_L'^2(t)}} \quad (6)$$

where $\langle v_L'^2 \rangle$ is used to normalize the equation. Equation (3) can now be written as

$$\sigma_y^2(t) = \overline{2v_L'^2} \int_0^t \int_0^\eta R_{v_L}(\tau) d\tau d\eta \quad (7)$$

From integration by parts of (7), Kampé de Fériet (1939) derived the following equation:

$$\sigma_y^2(t) = \overline{2v_L'^2} \int_0^t (t-\tau) R_{v_L}(\tau) d\tau \quad (8)$$

In order to calculate $\sigma_y^2(t)$, the integral in (8) must be known. The integral can be approximated by

$$\int_0^\infty R_{v_L}(\tau) d\eta = T_L \quad (9)$$

where T_L is the Lagrangian integral time scale. Equation (8) for long diffusion time may be expressed as

$$\sigma_y^2(t) \cong \overline{2v_L'^2} T_L \quad (10)$$

Evaluations of $R_{V_L}(\tau)$ and T_L were done for the Magna station in the Salt Lake Valley and are presented in Chapter 6, Results and Conclusions.

With the advent of the Fast Fourier Transform algorithm, a more useful and informative method of determining the diffusion parameters was found. This method involves the use of the power spectrum, $S_V(\omega)$ of the Eulerian wind speed v_E . Equation (11) shows the relationship of $S_{V_L}(\omega)$ to $R_{V_L}(\tau)$ and $\sigma_y^2(t)$.

$$S_{V_L}(\omega) = \frac{\sigma}{\pi} \int_0^{\infty} R_{V_L}(\tau) \cos \omega \tau d\tau \quad (11)$$

With much manipulation,

$$\sigma_y^2(t) = 2t^2 \int_0^{\infty} S_{V_L}(\omega) \left(\frac{\sin \omega t}{\frac{\omega t}{2}} \right)^2 d\omega \quad (12)$$

Equation (12) shows the diffusion parameters can be found by knowing only the spectrum and the diffusion time of interest.

The data that is used in this study was gathered at fixed stations which is the Eulerian system. However, (10) and (12) are in the Lagrangian system. The Equations (10) and (12) must now be converted into the Eulerian system.

Pasquill (1961) found that for the microscale, the Lagrangian and Eulerian time scales are related by

$$B \equiv \frac{T_L}{T_E} \approx 20 \quad (13)$$

For large diffusion time in the Eulerian system (10) may be expressed

as

$$\sigma_y^2(t) \cong 2\overline{v_E'^2} B T_E \quad (14)$$

and (12) expressed in terms of the spectrum of the Eulerian wind speed

$$\sigma_y^2(t) = 2t^2 \int_0^\infty S_{v_E}(\omega) \left(\frac{\sin \frac{\omega}{2} \left(\frac{t}{B} \right)}{\frac{\omega}{2} \left(\frac{t}{B} \right)} \right)^2 d\omega \quad (15)$$

For the wind speed and SO_2 we want to determine where the energy is located and what is the rate of dissipation in the higher frequencies. This information will give a more concise understanding of the $S_{v_E}(\omega)$ in (15) and help in forecasting the SO_2 spectra from the wind speed spectra which will ultimately lead to improved forecasting of SO_2 concentrations at different locations.

With equations (14) and (15), good values of $\sigma_y^2(t)$ or $\sigma_z^2(t)$ should be obtained providing homogeneous and stationary turbulence exist. These conditions do not exist in the large scale in either the Salt Lake Valley or in St. Louis, so many realizations must be taken under differing stability conditions to evaluate how the auto-correlation coefficients and the spectra behave. With many relations, quasi-stationary turbulence can be assumed for a given stability condition and the statistical theory can be applied to forecasting pollution concentrations.

CHAPTER 3

METHODS OF CALCULATION

$$\underline{R_{VE} \text{ and } R_{CE}}$$

The most important variable in Taylor's diffusion equation is the autocorrelation function R_{CE} or R_{VE} and how it varies with changing time lag. The classical method for calculating R_{VE} is

$$R_{VE} = \frac{\frac{1}{N} \sum_{i=1}^N u'_i(t) u'_i(t+\tau)}{\frac{1}{M} \sum_{i=1}^M \overline{u_i'^2(t)}} \quad (16)$$

where M is the length of the interval from which R_{VE} is calculated. Box and Jenkins (1970) suggest the following method:

$$R_{VE} = \frac{\sum_j^N u'_j(t) u'_j(t+\tau)}{\left[\sum_j^N u_j'^2(t) \sum_j^N u_j'^2(t+\tau) \right]^{1/2}} \quad (17)$$

where $N=n-\tau$ and n is the number of observations. Figure 1 shows R_{VE} calculated for the wind speed at Magna under neutral conditions. Note the values of R_{VE} for the classical method are slightly lower than that for the Box and Jenkins Method, however, the shape of the curve is similar.

Two types of averages were used in this study, the 24 hour

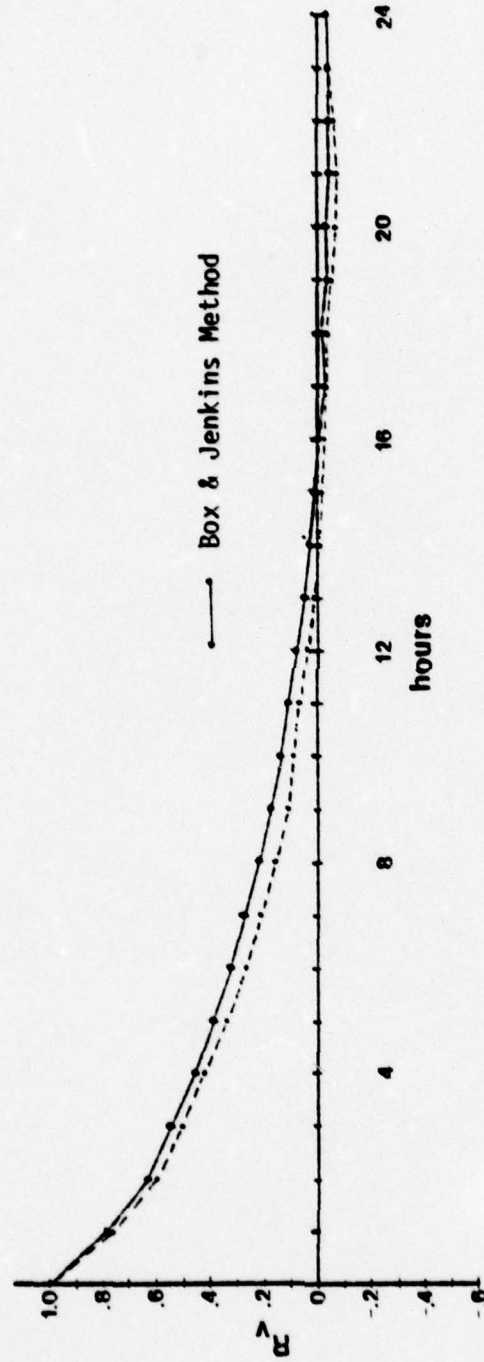


Figure 1. Auto-correlogram of the wind speed at Magna under neutral conditions.

moving average and eliminating the linear trend.

The 24 hour moving average was calculated using

$$\bar{u}_j = (0.5 u_{j-12} + \sum_{i=-11}^{11} u_{j+i} + 0.5 u_{j+12})/24 \quad (18)$$

where u_{j+12} and u_{j-12} are the values plus and minus 12 hours from the u_j in question. A \bar{u}_j is calculated for every point in the realization and u'_j is found by

$$u'_j = u_j - \bar{u}_j \quad (19)$$

The linear trend was the other method used to calculate \bar{u}_j . Any steady increase or decrease in concentration or wind speed which prevailed throughout the entire realization is eliminated. Equation (19) is then used to calculate u'_j .

The Spectrum

J. N. Rayner (1971) outlines a direct method to calculate the spectrum. I have used this method and modified it slightly to accommodate spectral density and ensemble averaging calculations. See Appendix B for computer programs.

The first step of the direct method is to remove the linear trend. Since periods as short as three days in the Salt Lake data and one day in the St. Louis data are used, any wave longer than three days or one day, respectively, will be affected by this trend removal and might not produce meaningful results.

Once the trend was removed, a cosine bell window function was multiplied to the first and the last ten percent of the data in the

following manner. For the first ten percent of the data, the window function (20) is used.

$$h[j] = \frac{1}{2} \left\{ 1 - \cos \frac{\pi j}{G} \right\} \quad 0 \leq j \leq G \quad (20)$$

where $h[j]$ is the window function, D is the length of the time series, $G = D/10$, and j is the data hour. For the last ten percent, the descending cosine bell window function is

$$h[j] = \frac{1}{2} \left\{ 1 - \cos \left[\frac{\pi(D-j)}{G} \right] \right\} \quad D - G < j \leq D - 1 \quad (21)$$

The third step is to add zeros to both ends of each time series. This is done for two reasons: one, to correct for the non-periodicity of the time series, and two, to make all the realizations the same length of 336 hours so the frequency resolution will be equal and thereby allow ensemble averaging.

The fourth step is to call the Fast Fourier Transform (FFT) algorithm. The basic equation in the algorithm is

$$V(n) = \sum_{j=0}^{N-1} v([j+1]\Delta t) e^{-2\pi i j \Delta t / N \Delta t} \quad (22)$$

where $V(n)$ is the complex Fourier coefficient, $v([j+1]\Delta t)$ is the value of either wind speed or SO_2 concentration in the time series, and $N\Delta t$ is the length of the time series. A real time series is input into the FFT subroutine which calculates $N/2$ complex Fourier coefficients. The $(N/2+1)$ th Fourier coefficient is calculated separately and in this analysis contains the amplitude at the frequency 0.5 cycles/hour.

After the FFT subroutine has provided the complex Fourier

coefficients, Equation (23) calculates the power spectrum with an elementary band width of 0.00298 cycles/hour. The power spectrum is

$$E_V(n) = \frac{1}{2}|V(n)|^2 \quad (23)$$

for all n from 1 to $N/2+1$.

The fifth step is to calculate the normalized spectral density by dividing the spectrum of each realization by the variance for that realization.

Finally, each frequency is ensemble averaged. The result is the normalized spectral density for one case and location.

Chapter 4

DATA

Salt Lake City Vicinity

Of the two metropolitan areas selected for this study, the Salt Lake Valley and surrounding areas have much more rugged terrain, Figure 2. Four air pollution monitoring sites were used. The stations are located at Magna, Kearns, Tooele and Bountiful.

Sulfur dioxide (SO_2) is the effluent monitored in this study. It was chosen because of its long half life and the relatively high concentrations at the four sites. The major single SO_2 source in the Salt Lake area is the Kennecott Copper Corporation smelter located at the north end of the Oquirrh Mountains (Kao and Taylor, 1977). Since the Kennecott smelter is a major source of SO_2 , especially near the Magna, Kearns and Tooele sites, it is assumed to be a point source. Also, the rate of effluent emission is assumed to be constant throughout each realization, but the rate may vary from realization to realization. This variance is of no consequence since deviations from the mean or trend are calculated.

St. Louis

St. Louis is a large metropolitan area located on relatively flat terrain near the Mississippi River just south of the confluence of the Missouri and Mississippi Rivers. Figure 3 shows the monitoring stations and the major SO_2 sources affecting the stations.

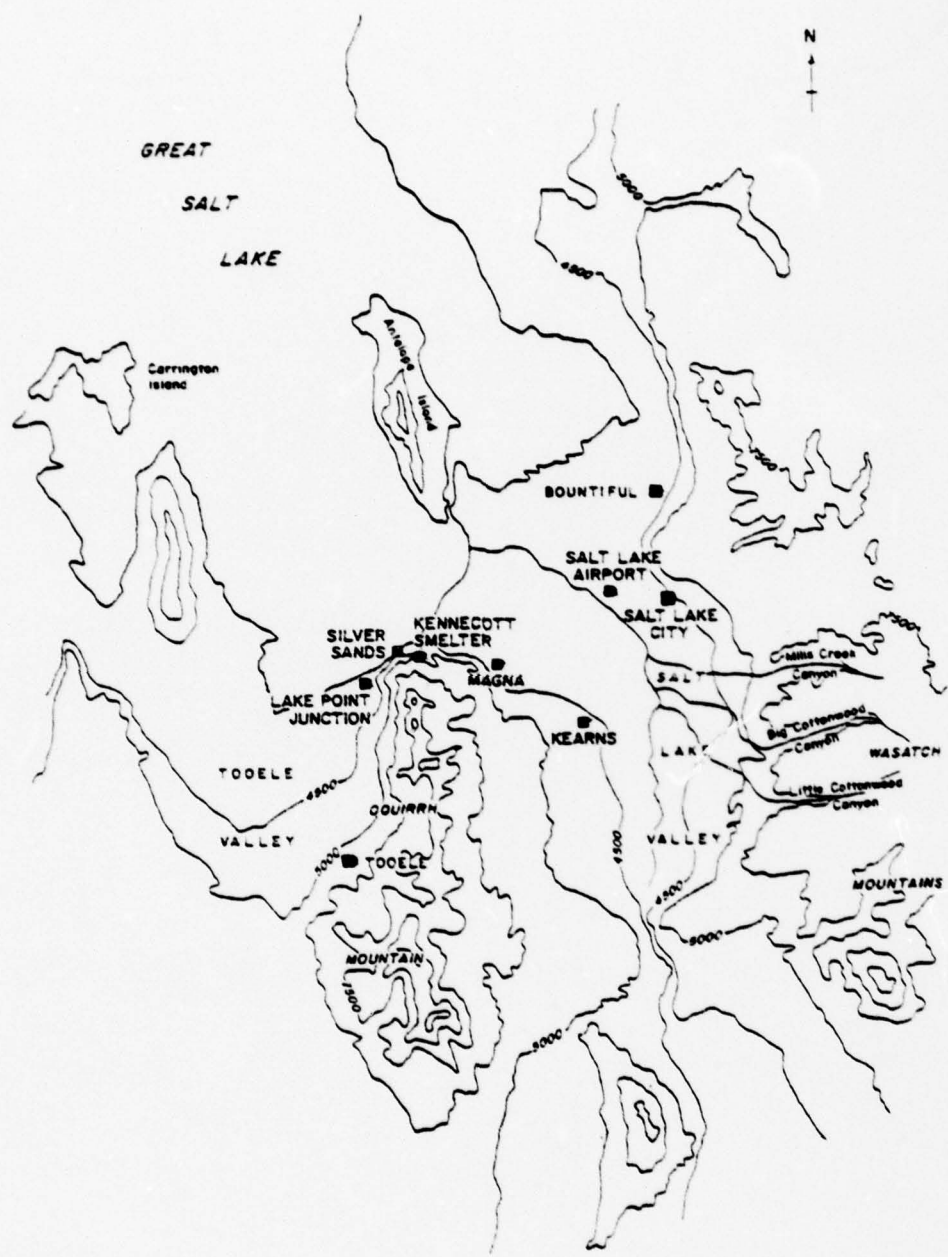


Figure 2. Base map of the Salt Lake Valley and Vicinity.

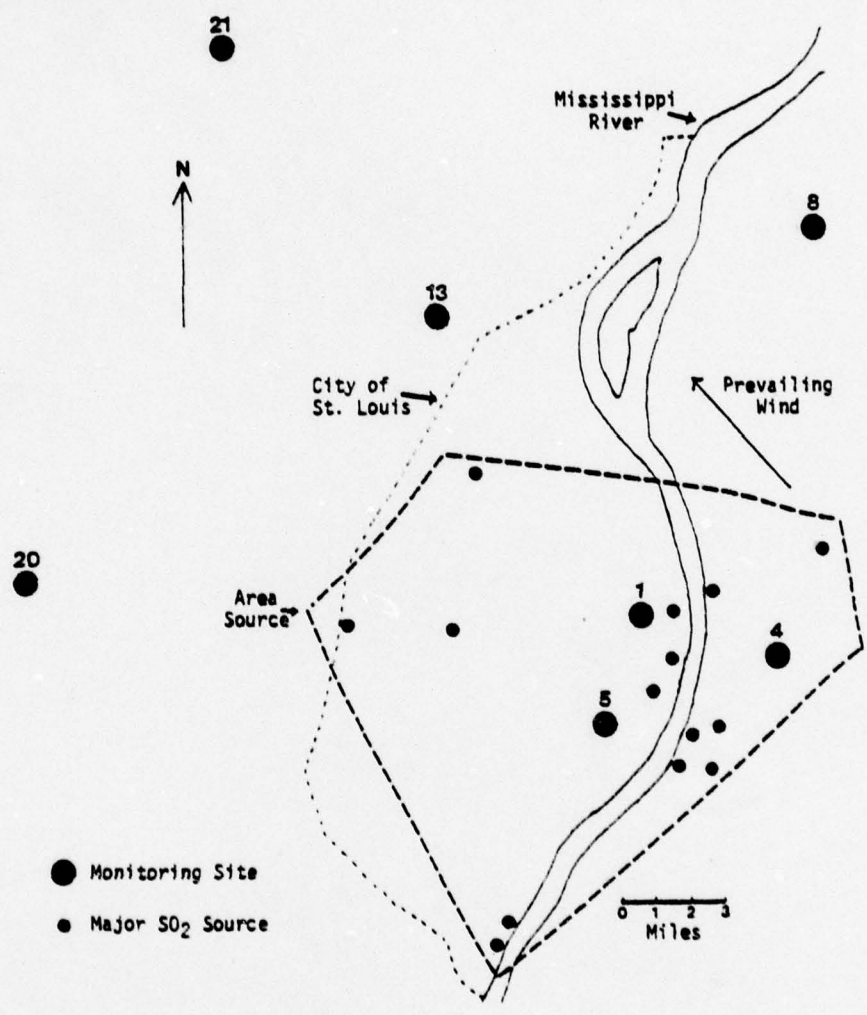


Figure 3. Base map of St. Louis.

With the high number of SO_2 sources, the only assumption to make is the area outlined in Figure 3 be considered an area source and contains the majority of SO_2 effluent (Littman et al., 1976). Again, the rate of effluent emission is assumed to be constant throughout each realization.

Monitoring Equipment

The Salt Lake City vicinity stations are operated and maintained by the Utah State Division of Health, Bureau of Environmental Health-Air Quality Section. The St. Louis stations are operated and maintained by the Environmental Protection Agency.

The anemometers used at all sites in the Salt Lake City vicinity and St. Louis were standard rotating cup anemometers. The make of the instruments varied, but all have a threshold of approximately one meter per second with an instantaneous error of ± 0.5 meters per second.

The SO_2 monitors vary in type and method of operation, but all have a threshold of 0.005 parts SO_2 per million (ppm) and an accuracy of ± 0.005 ppm. The types and heights above the surface, of the anemometers and SO_2 monitors follow:

Magna: Type SO_2 monitor: flame photometric.

Height above surface: 30-foot tower.

Kearns: Type SO_2 monitor: conductimetric.

Height above surface: 24-foot tower on a one-story building.

Tooele: Type SO_2 monitor: conductimetric.

Height above surface: 24-foot tower on a one-story building.

Bountiful: Type SO_2 monitor: conductrimetric.

Height above surface: 24-foot tower on a one-story building.

St. Louis: Type SO_2 monitor: all flame photometric.

Height above surface: 30-meter free-standing tower at all sites except Site 8 which has a 10-meter free-standing tower.

Averaging

All the data used in this study is hourly averaged. Salt Lake City vicinity station averages are obtained by polling the instantaneous wind speed or SO_2 concentration once every six minutes, averaging the values, and rounding to the nearest whole mph or 0.01 ppm, respectively. The St. Louis station averages are obtained by polling the instantaneous wind speed or SO_2 concentration once every minute, averaging the values, and rounding to the nearest 0.01 m sec or 0.0001 ppm.

Pasquill (1962) explains the effect of averaging on the spectra. Two problems arise in the averaging process. The first is to reduce the fraction of the total variance that appears in the higher frequencies. The second is to introduce aliasing.

In this study, the fraction of total variance lost in the higher frequencies does not become significant except for frequencies greater than 0.4 cycles/hour (Table 1). This region of the spectra is small compared to the total domain.

When observations are at discreet intervals, and in this study the interval is one hour, the variations associated with oscillations

Table 1
Effect of Hourly Averaging on Spectral Variance

Frequency (cycles/hour)	Fraction of Variance Remaining
0.1	0.97
0.2	0.88
0.3	0.80
0.4	0.62
0.5	0.45

greater than 0.5 cycles/hour appear at a lower frequency. This source of error is called aliasing. If aliasing is a problem, the spectra will show high amplitudes in the frequency range greater than 0.3 cycles/hour. The Bountiful wind speed spectra, but no other, show the high amplitudes and the reason for the high amplitudes will be discussed in Chapter 6.

Chapter 5

STABILITY CATEGORY DETERMINATION

Stability Indices

One of the major problems in the air pollution meteorology field is determining the stability of the atmosphere in the surface and planetary boundary layer. Three major causes of this problem are diurnal stability fluctuations at a single location, horizontal homogeneity of stability, and variations in stability among cases that have the same synoptic situations. Since these problems exist, methods of classifying periods into similar groups are necessary if any analysis of SO₂ and wind speed fluctuations are to yield meaningful information.

The Salt Lake Valley and St. Louis have different topography and thus differing stability problems. Because the valley effect poses unique problems, the National Weather Service Forecast Office in Salt Lake City has developed a method of determining stability classifications for the Salt Lake Valley. However, St. Louis uses nationally produced air quality classification products.

The differences in mixing depths, wind speeds and air pollution potential between Salt Lake City and St. Louis was found by Holzworth (1967). He found that throughout the year, the height of the mixing depth in the morning averages 200 feet lower in the Salt Lake Valley than at St. Louis. The average wind speed in the morning

for Salt Lake City was about two meters per second slower every month than at St. Louis. The afternoon monthly average wind speeds were about four meters per second slower during the winter months at Salt Lake City and about equal during the summer. The air pollution potential was about equal on the average even though the Salt Lake City size was only half the city size of St. Louis.

Since 1967, the National Weather Service Forecast Office at Salt Lake City has calculated daily an Air Stagnation Index (ASI) which incorporates the height of the mixing depth, mean wind speed through the mixing depth and surface temperature (Jackman and Chapman, 1977). The ASI was used to determine the stability category for the Salt Lake and adjacent valleys.

Seventy-eight percent of the stagnant high pressure areas in the Salt Lake area occur during the months of November through February (Jackman, 1968). Since the stable periods are of most interest, cases were only selected from these months.

Jackman and Chapman (1977) found conditions in the Salt Lake Valley can be separated into three categories during November through February (the winter months). These categories are $ASI < 200$, $200 < ASI < 1,000$ and $ASI > 1,000$, and are used throughout the Salt Lake Valley analysis.

The first category $ASI < 200$ is called the stable case. This condition occurs when cold air trapped in the valleys combined with radiation and snow cover, results in strong surface inversions. Usually, warm air advection above the inversion tends to strengthen the stable condition at the surface. This stagnant layer is generally confined to below 6,000 feet. Under these conditions, diurnal

heating is unable to destroy the stable layer making the mixing depth very shallow. Winds below the inversion are very light and often show a diurnal reversal limiting any horizontal transport (Kao, Lee and Smidy, 1975).

The second category, $200 < \text{ASI} < 1,000$ is called the neutral case. In this range, synoptic conditions are generally characterized by a subsidence inversion or stable layer between about 6,000 and 12,000 feet. Surface heating usually allows mixing to the base of this stable layer which gives a moderate mixing depth in the valley. However, the base of the stable layer may be at or just above higher mountain areas, and may severely restrict the vertical transport of pollutants.

The third category, $\text{ASI} > 1,000$ is called the unstable case. The vertical temperature lapse rate approaches the dry adiabatic rate. Mixing depths can extend to great heights, especially in the presence of approaching frontal systems.

The category determination for St. Louis was not as quantitative as the Salt Lake City categories because no localized pollution index was available. The data was divided into two categories, stable and neutral. No unstable category was used because under the unstable conditions, most of the SO_2 concentrations were zero. Data was placed in the stable category if St. Louis was under a stagnant high pressure area, the vast majority of the hourly wind speeds were below three meters per second and the hourly wind directions were between 090° and 180° . Data was placed in the neutral category if no stagnant high pressure was over the St. Louis area, no precipitation was recorded, the vast majority of the hourly wind speeds were between three and six

meters per second, and the hourly wind directions were between 090° and 180° .

Quantity of Data

Data for the Salt Lake Valley cases was taken from 1970 to 1977 during the months of November through February. If a period of three consecutive days or longer with the same stability category was found, then the period qualified as a realization for the respective stability category.

At Magna, both SO_2 and wind speed data was used. For Magna, stable, 23 realizations were used with lengths between three and 13 days. For the neutral case, 29 realizations were taken ranging from three to eight days. For the unstable case, 17 realizations were found varying in length from three to six days.

At Kearns and Tooele, only SO_2 data was available during stable periods. Eighteen cases at Kearns and 11 cases at Tooele were found. All cases varied in length from three to 13 days.

Bountiful had sufficient data to calculate both stable and neutral wind speed and SO_2 spectral densities. For the stable case, 18 realizations with lengths of three to 13 days, and for the neutral case, 10 realizations of length three to five days were found.

The data used in the St. Louis calculations varies from the Salt Lake data in some respects. Since only 1976 data was available, realizations were taken from any month of the year. When 24 consecutive hours or more were found with wind direction, speed and synoptic conditions meeting the above stated criteria, the period qualified for use.

The seven St. Louis stations had the same realizations. Stations 1, 4, 5 were grouped together and called urban stations because of their location. Stations 8, 13, 20 and 21 were grouped and called suburban stations. For the stable case, nine realizations of SO_2 and wind speed were used. For the neutral case, 16 realizations were found. All realizations varied in length from one to three days.

Since the realization length is much shorter for St. Louis cases compared to Salt Lake Valley cases, the lower frequency waves in the St. Louis spectra will be suppressed. This fact can be seen by noting the spectral densities of both areas in Chapter 6.

Degrees of Freedom

Rayner (1971) gives a method of estimating the degrees of freedom for each realization. The following all affect the degrees of freedom: the number of points tapered at each end of the realization, G ; the length of the realization, D ; the elementary bands, $n/2$; and the number of elementary bands in non-overlapping groups, B . An equation to estimate the degrees of freedom, ν , is

$$\nu \approx \frac{B(D-G)}{n/2} \quad (24)$$

where G is 10 percent of D .

Since the degrees of freedom for each realization in a stability case are summed, the D and G in Equation (24) are the sum of all the realization lengths and tapered points, respectively.

The degrees of freedom vary for the same spectrum because the number of elementary bands in non-overlapping groups increase with increasing frequency. Only one elementary band is in the groups from

0.003 to 0.065 cycles/hour, two bands in the groups from 0.065 to 0.119 cycles/hour, five bands in the groups from 0.119 to 0.298 cycles/hour and ten bands in the groups from 0.298 to 0.500 cycles/hour.

The degrees of freedom for the shortest and longest time series were calculated. For the St. Louis urban case, which is the shortest time series, the degrees of freedom are 5.2 for the 0.003 to 0.065 cycles/hour range increasing to 52 for the 0.298 to 0.500 cycles/hour range. For the Magna neutral case, which is the longest time series, the degrees of freedom are 15.7 for the 0.003 to 0.065 cycles/hour range increasing to 157 for the 0.298 to 0.500 cycles/hour range.

Chapter 6

RESULTS AND CONCLUSIONS

Auto-correlograms

Autocorrelation coefficients were calculated only for Magna since the spectra yields more information than auto-correlograms. Some interesting conclusions can be drawn from the auto-correlograms, however. The autocorrelation coefficients of SO_2 and wind speed under three thermal stability conditions were investigated for their similarities and differences.

The auto-correlogram under stable conditions using the 24 hour moving average shows very similar coefficients between SO_2 and wind speed up to a lag of 13 hours, (Figure 4). The coefficients of SO_2 damps out for longer time lags, but that of the wind speed continues to show relatively high values of 0.3 and 0.2 at 24 and 48 hours respectively. This correlation which shows the diurnal effects of the wind speed in the Salt Lake Valley during stable conditions could be a consequence of the effect of lake-valley circulation.

In the neutral case the similarity between SO_2 and wind speed auto-correlograms (Figure 5) is less than in the stable case. In the time lag of the first five hours the area under the curve is greater for SO_2 than wind speed. No diurnal correlation shows in the wind speed. This is due to wind speeds being less

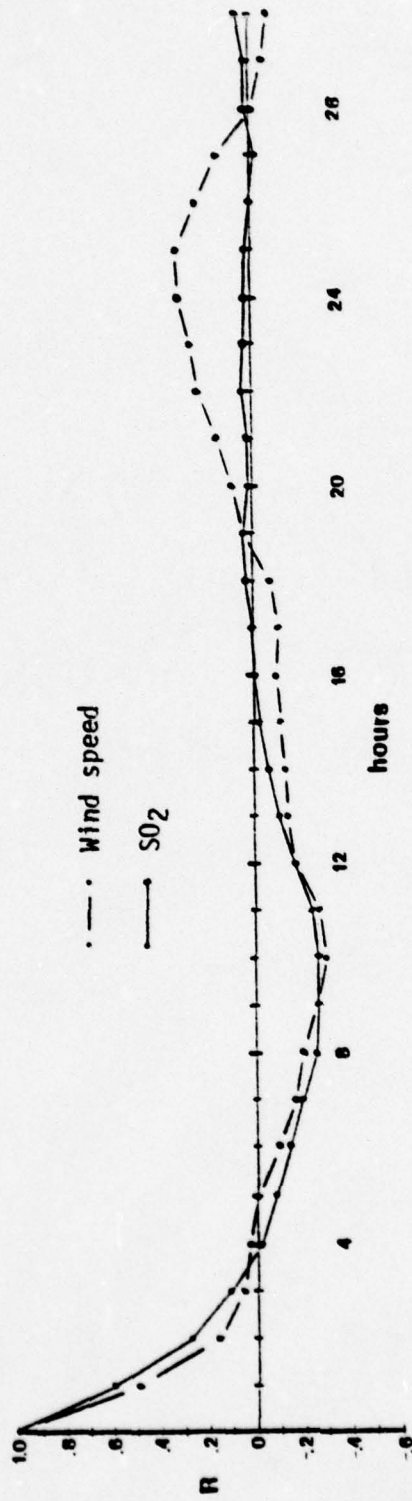


Figure 4. Auto-correlogram of Magna under stable conditions using a 24 hour moving average.

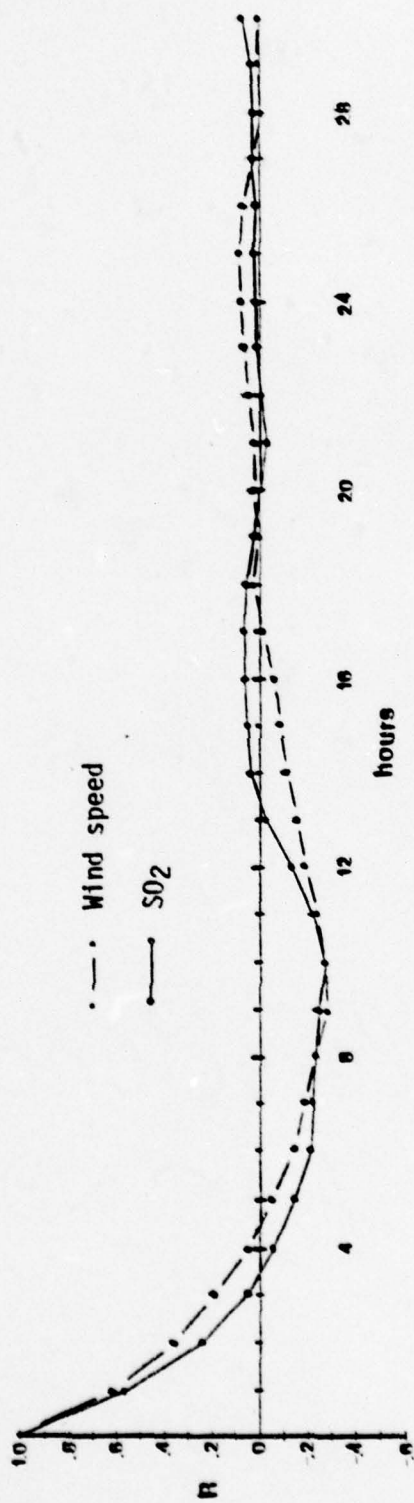


Figure 5. Auto-correlogram of Magna under neutral conditions using a 24 hour moving average.

affected by diurnal circulation in neutral periods.

With unstable conditions less similarity exists between SO_2 and wind speed auto-correlograms than in neutral conditions in time lags less than five hours, (Figure 6). Again, no diurnal variation is apparent in the wind speed correlation due to the intense vertical mixing.

A direct relationship exists between the integral area for time lag from zero to four hours, and the stability category (Figure 7) for SO_2 and an inverse relationship exists for wind speed. During the stable periods SO_2 concentrations are generally better correlated than those during neutral and unstable periods. With wind speed, higher correlations show in the unstable periods than in the neutral or stable periods.

Two similarities exist between all auto-correlograms. All autocorrelation coefficients go to zero between time lag of four to five hours when using the 24 hour moving average, and the negative correlations are very similar for all auto-correlograms, (Figure 7).

Two methods of calculating the autocorrelation coefficients were employed, the 24 hour moving average and eliminating the linear trend. Each method has its usefulness. By comparing Figure 7 with Figure 8 it can be seen that using the 24 hour moving average to calculate the autocorrelation coefficients gives the best similarity in the auto-correlograms of the hourly averaged data among stability categories for both wind speed and SO_2 . If only the linear trend is eliminated, then the differences

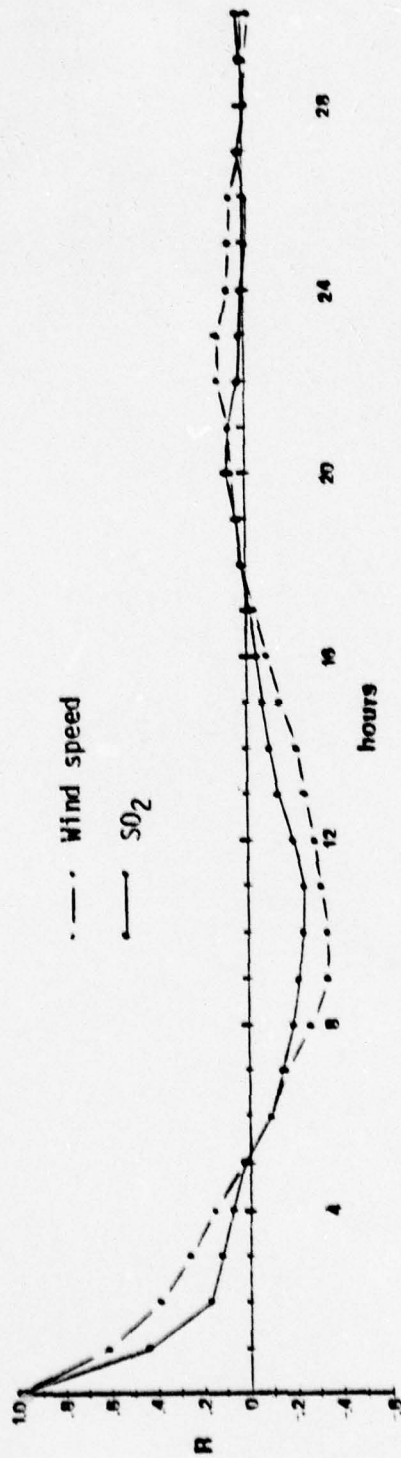


Figure 6. Auto-correlogram of Magna under unstable conditions using a 24 hour moving average.

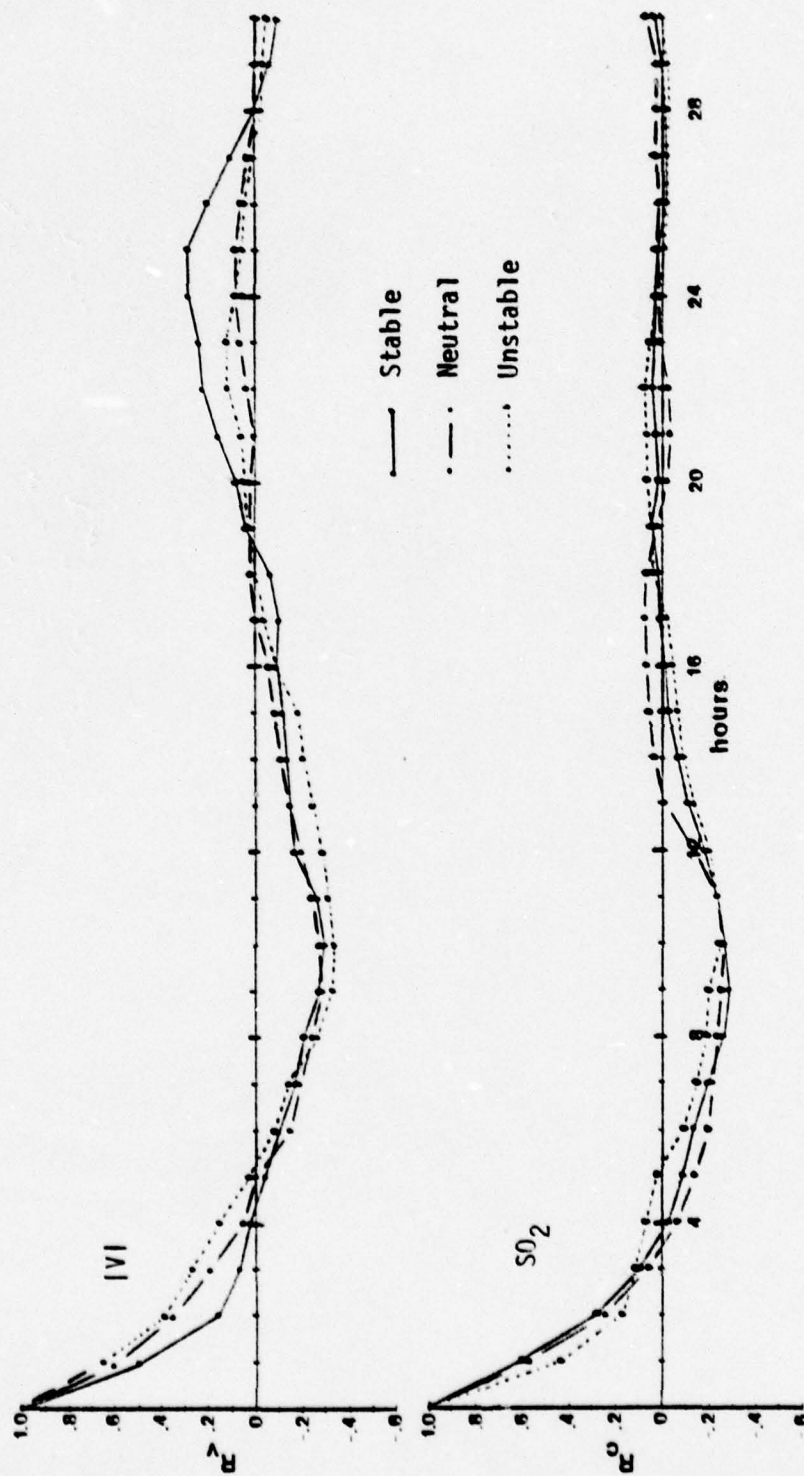


Figure 7. Auto-correlogram of Magna using a 24 hour moving average with wind speed (top) and SO₂ (bottom).

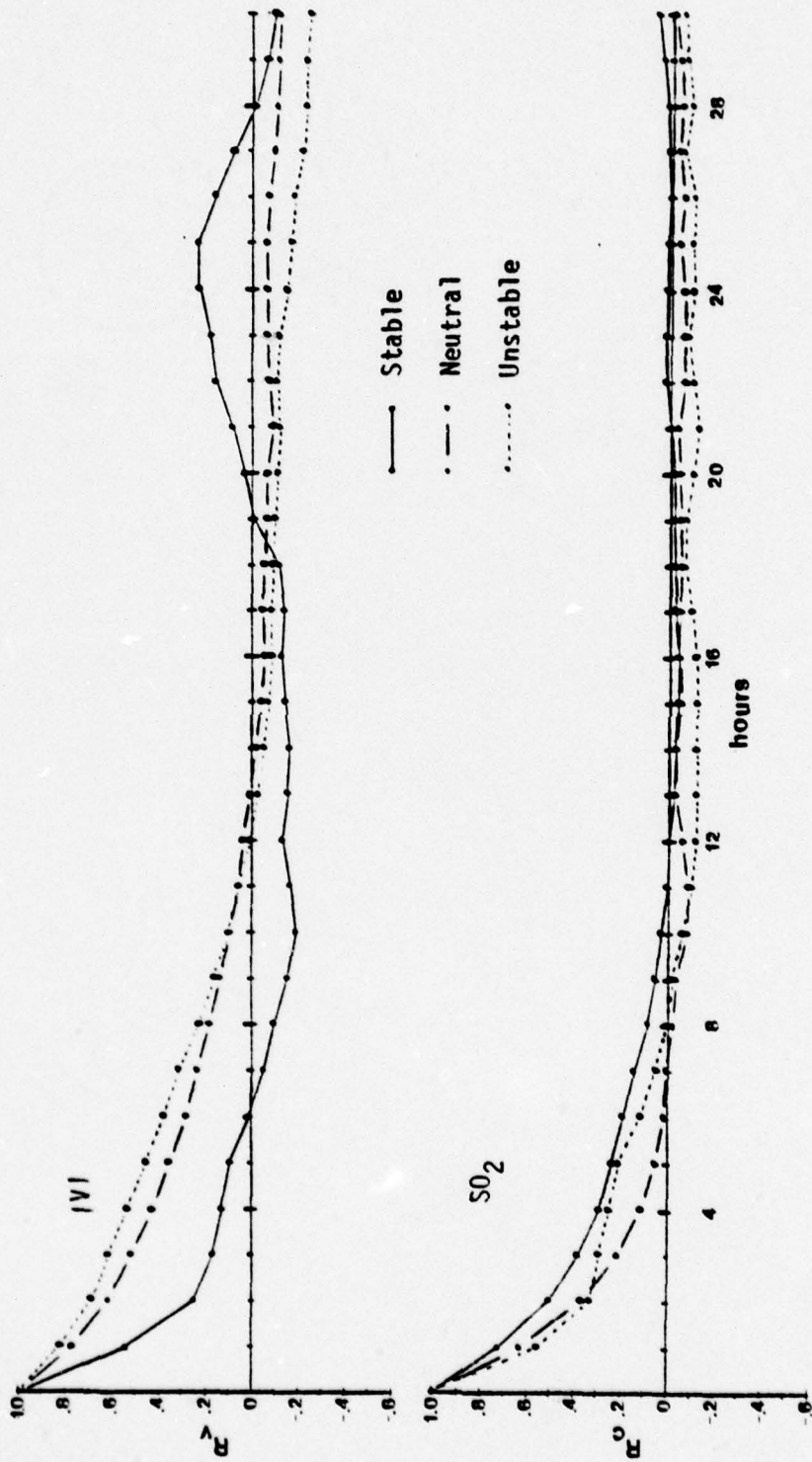


Figure 8. Auto-correlogram of Magna after eliminating the linear trend with wind speed (top) and SO_2 (bottom).

in the integral time scales among the stability categories will be larger. This makes for easier comparison among auto-correlograms for different stabilities.

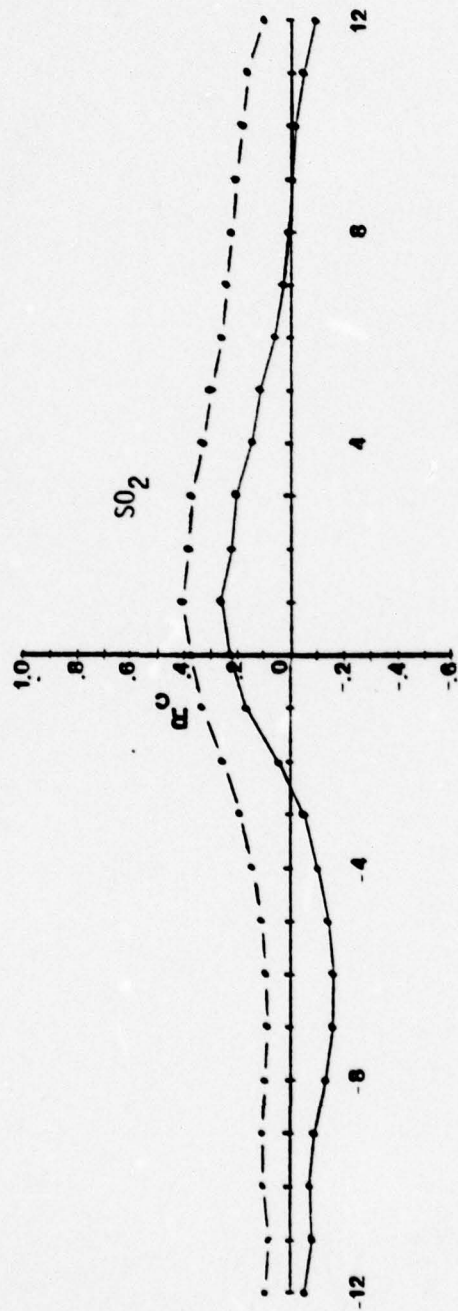
Cross-correlograms

Cross-correlograms can provide useful information about correlations between different stations. The cross-correlogram in Figure 9 shows correlations of SO_2 between Magna and Kearns. The maximum correlation of 0.42 occurs at a lag of one hour when the $v_E'(t)$ is calculated from the Magna data and the $v_E'(t+\tau)$ is from the Kearns data. This result shows that often a change in concentration at Magna will appear at Kearns one hour later. This occurrence is expected since Kearns is further down wind from the major pollution source. A second interesting correlation appears at a lag of 26 and 27 hours. This shows a probable diurnal relationship. It will be shown in the discussion of the SO_2 spectra in stable periods that a diurnal variation exists.

Comparison of SO_2 and Wind Speed Spectrum

The most important part of this study is analyzing the similarities of SO_2 and the wind speed spectra. It is the objective of this study that similarity between the spectra can be established so that the spectral density in varying spectral bands of the SO_2 spectrum can be predicted from the spectral density in the wind speed spectrum.

Since the Magna site provided sufficient data to analyze the spectra of SO_2 and wind speed for all three stability categories,



—•— 24 hour moving average
 - - -•- Linear trend eliminated

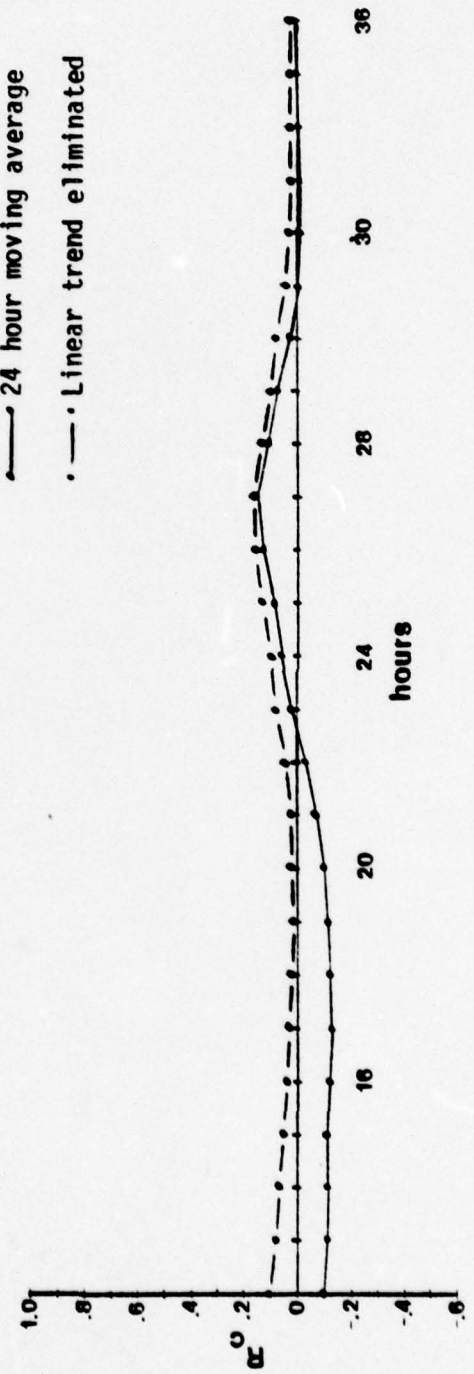


Figure 9. Cross-correlogram of Magna vs. Kearns under stable conditions.

we shall first analyze the spectra at Magna.

The SO_2 and wind speed spectra for stable periods were similar in general appearance, but the wind speed spectrum has more pronounced maxima, (Figure 10). In both spectra a broad maximum appears in the frequencies from 0.006 to 0.009 cycles/hours (periods of 168 to 112 hours). These low frequency waves are possible because 12 of the 23 realizations are five days or longer thereby allowing a wave of longer than 112 hours to appear. This maximum is more pronounced in the SO_2 spectrum than in the wind speed spectrum because the buildup of background SO_2 occurs over the course of at least three days during a stable period. Another broad maximum occurs in both spectra between 0.025 to 0.05 cycles/hour (period of 40 to 20 hours). This maximum encompasses the 24 hour diurnal period. The amplitude of the 24 hour period is especially strong in the wind speed spectrum and is probably due to the lake-valley circulation in stable periods. Also, two other peaks correspond in both spectra; the 0.083 and 0.125 cycles/hour peaks (12 hour and 8 hour periods). The 12 hour peak is probably due to a combined mountain-valley and lake breeze effect and will be discussed in more detail later. As with the other prominent peaks the 12 and 8 hour peaks are higher in the wind speed spectrum.

Unlike the 0.006 to 0.009 cycles/hour range where the SO_2 spectrum had a more pronounced maximum, all peaks with frequencies at higher than 0.04167 cycles/hour (24 hour period) show more pronounced maxima in the wind speed spectrum. This fact suggests that a different mechanism is affecting waves of period greater than 24 hours compared to less than 24 hours. Since the wind speed spectrum

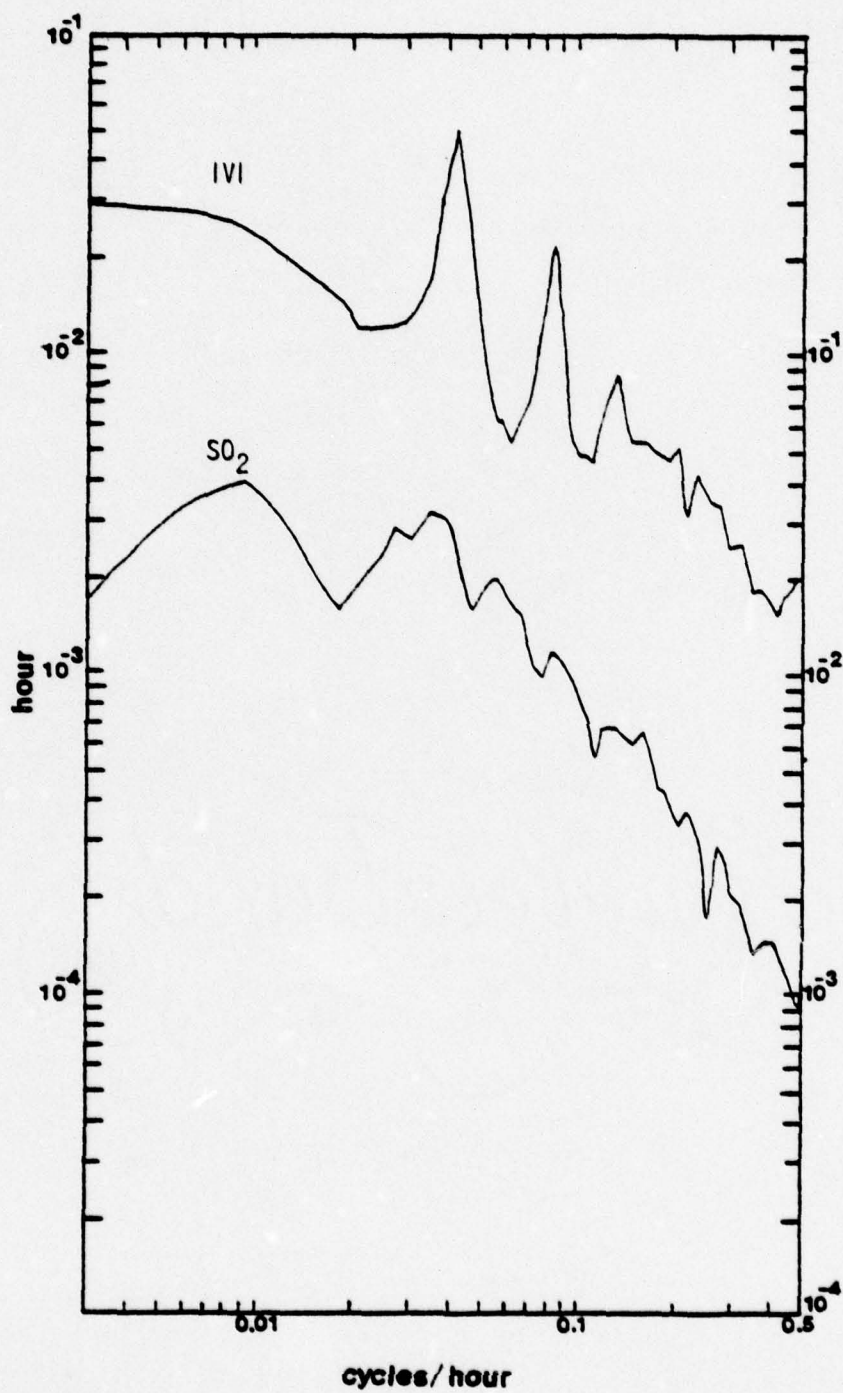


Figure 10. Normalized spectral density of Magna under stable conditions with wind speed (top) and SO₂ (bottom).

has the higher peaks in the frequencies equal to or greater than 0.04167 cycles/hour, it seems likely that in this frequency range the wind speed spectrum greatly affects the spectrum of SO_2 . But in the frequencies less than 0.04167 cycles/hour, the SO_2 spectrum is probably influenced more by the buildup of SO_2 trapped in the valley than by the wind speed.

The neutral and unstable spectra can now add more substantiation to the above claim, (Figures 11 and 12). For the neutral spectrum the wind speed shows a 24 and 12 hour maximum, but not as predominant as the wind in the stable category. The SO_2 neutral spectrum shows a weak maximum around 24 hours, but no 12 hour maximum. Both neutral SO_2 and wind speed spectra have a broad maximum centered around 0.01 cycles/hour. In the unstable case at Magna a weak peak appears around 24 hours, but no other significant peaks are evident. For SO_2 small peaks appear at 24 and 48 hours, but at no other frequency.

In the stable category, the wind speed and SO_2 spectra compare similarly, but the similarity decreases with increasing atmospheric instability suggesting that variables such as vertical motion and precipitation have more effect on the SO_2 spectrum than the horizontal wind speed.

This decrease in similarity between the SO_2 and wind speed spectra is also seen in the St. Louis urban spectra, (Figures 13 thru 16). The peak in the urban stable wind speed spectrum at 0.095 cycles/hour matches the SO_2 spectrum peak at 0.083 cycles/hour (12 hour period). The urban neutral wind speed has no peak in the 0.08 to 0.1 cycles/hour range, but a peak at 0.083 cycles/hour

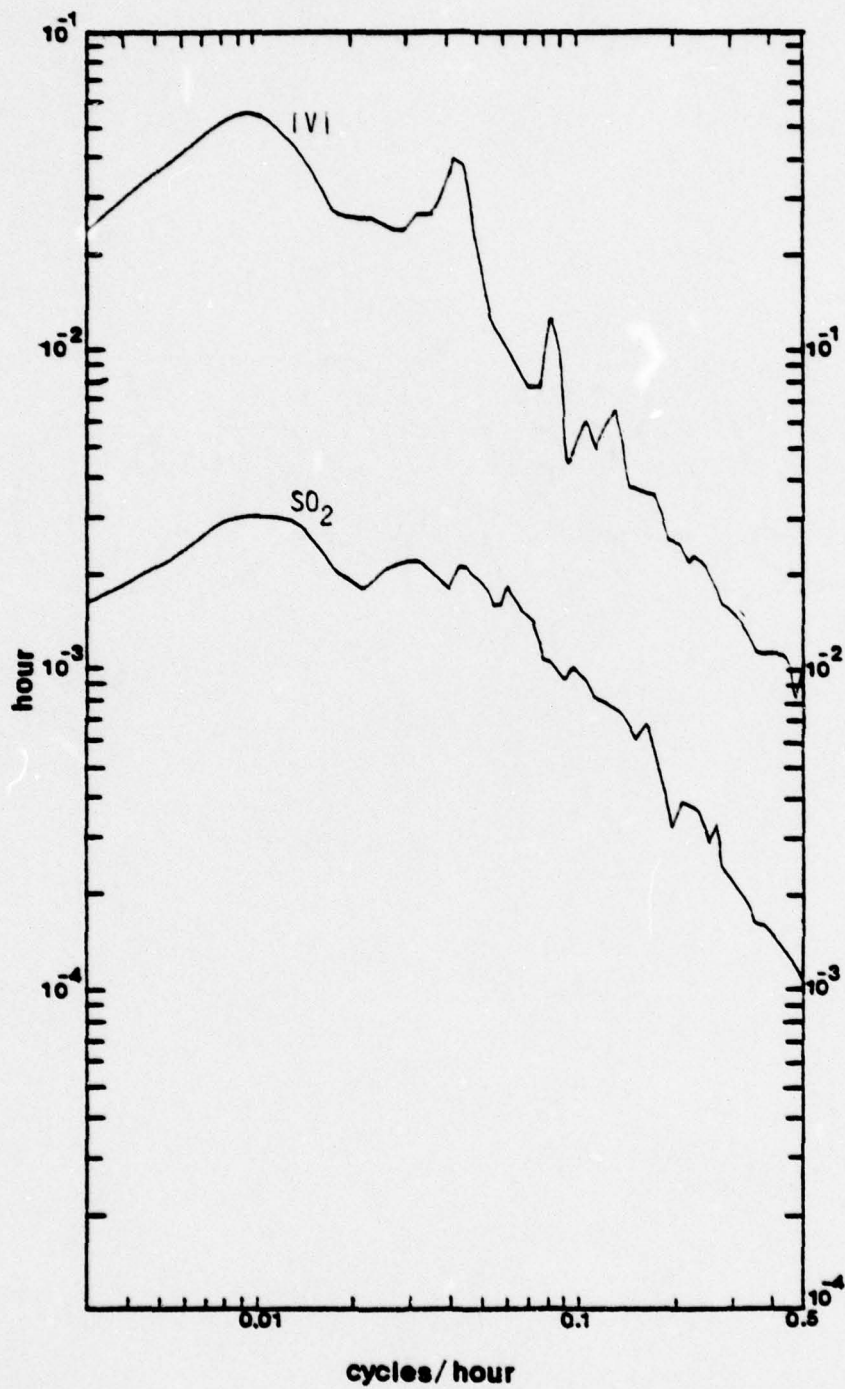


Figure 11. Normalized spectral density of Magna under neutral conditions with wind speed (top) and SO₂ (bottom).

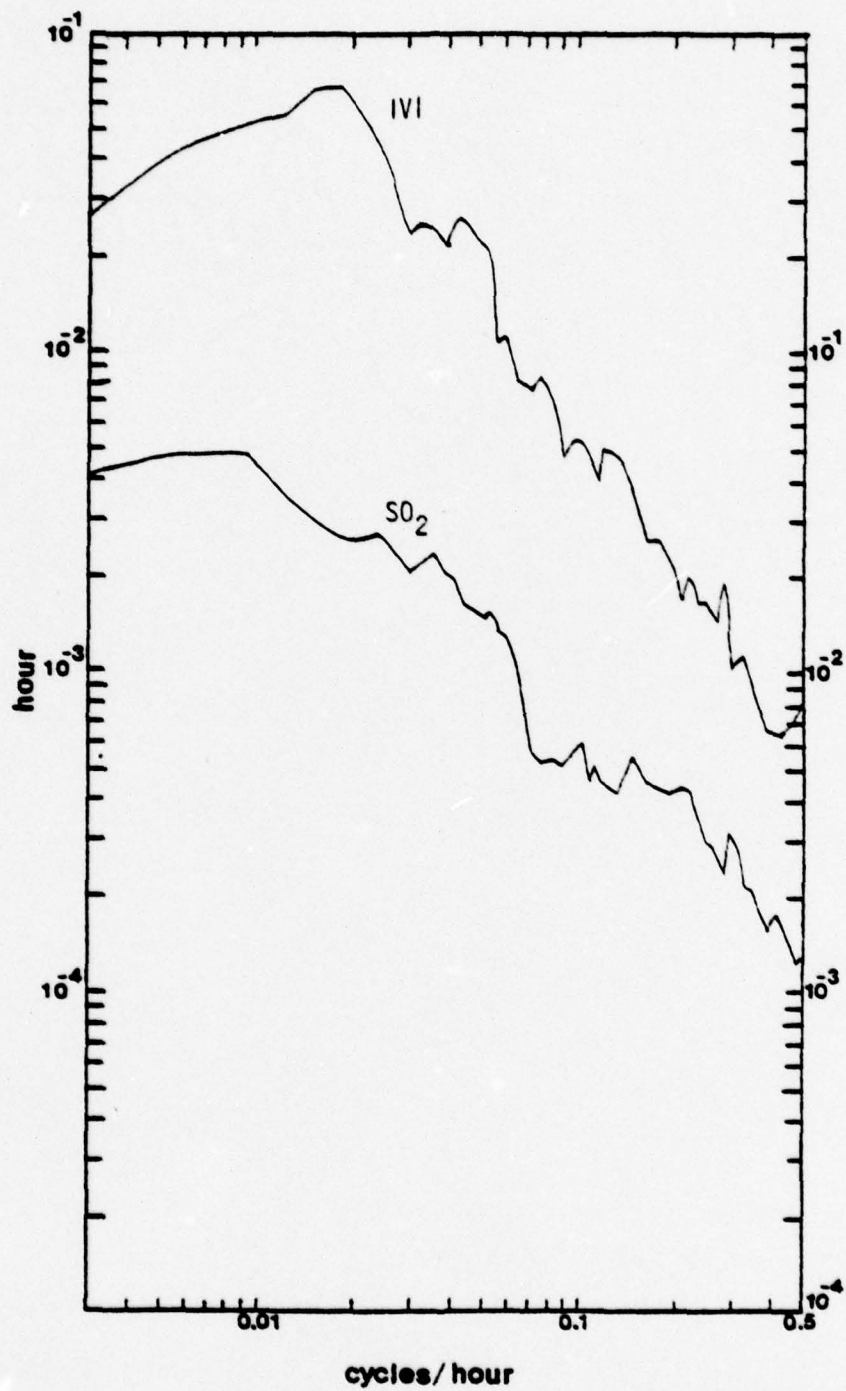


Figure 12. Normalized spectral density of Magna under unstable conditions with wind speed (top) and SO₂ (bottom).

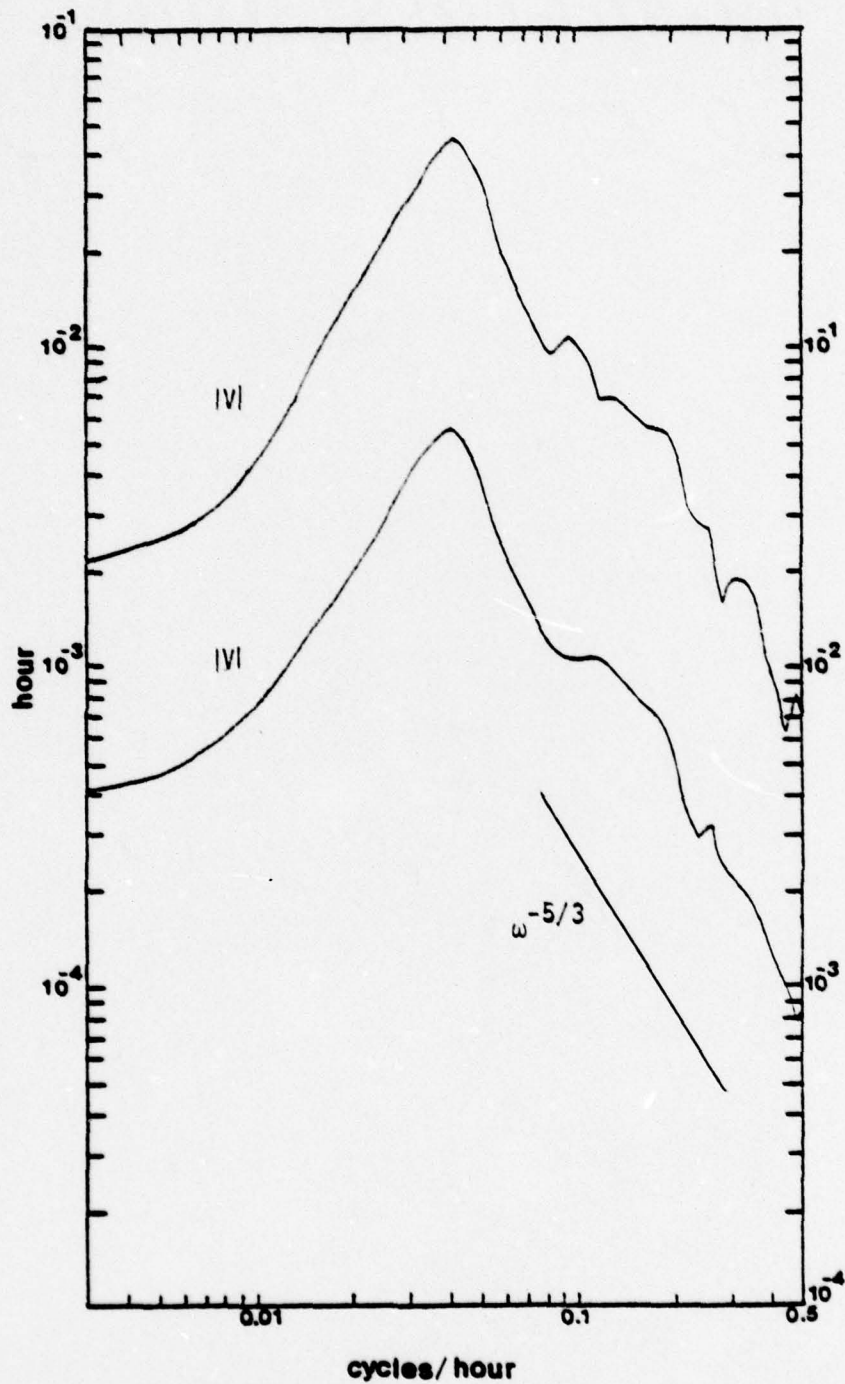


Figure 13. Normalized spectral density of the wind speed for urban St. Louis under stable conditions (top) and neutral (bottom).

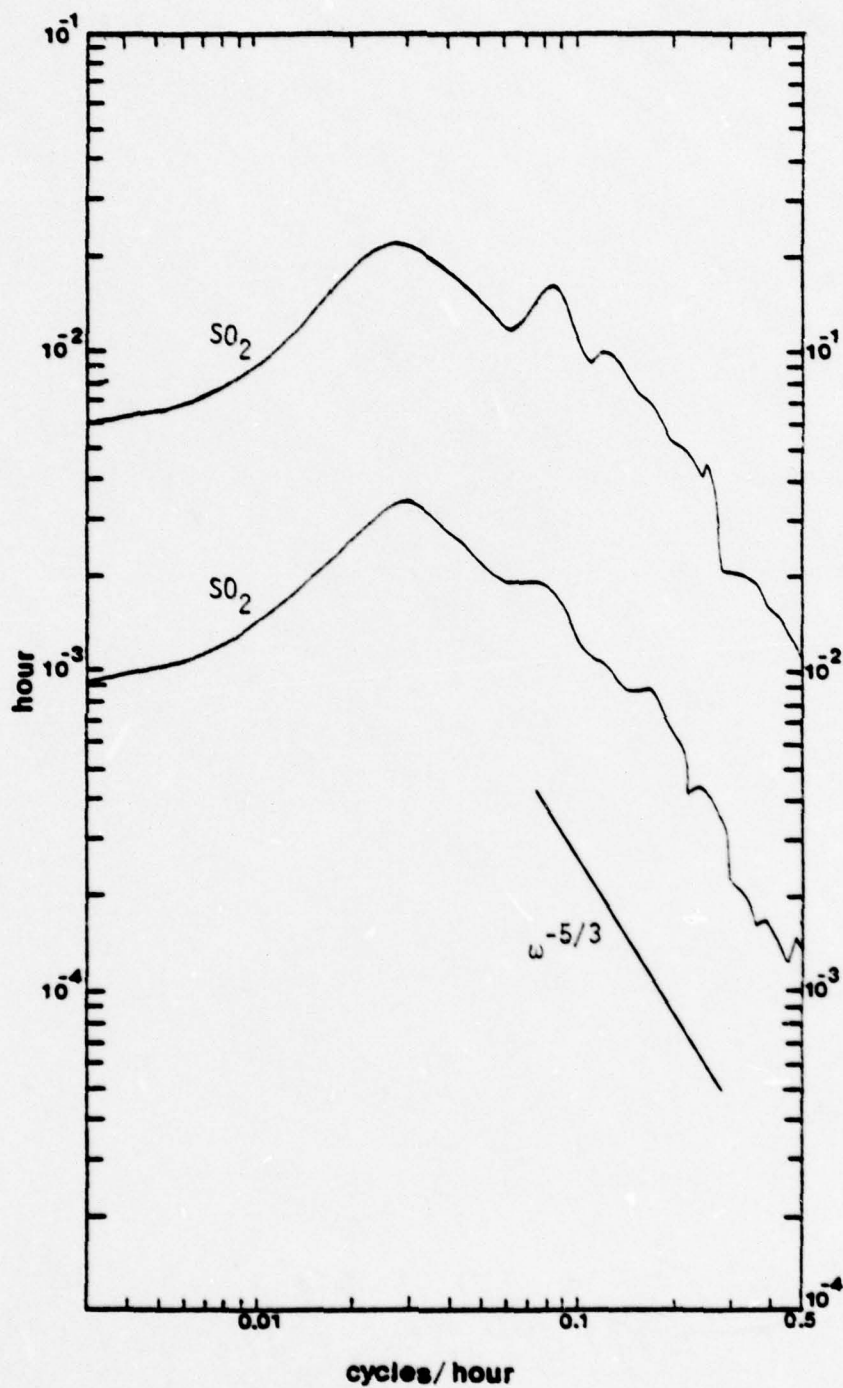


Figure 14. Normalized spectral density of the SO_2 for urban St. Louis under stable conditions (top) and neutral (bottom).

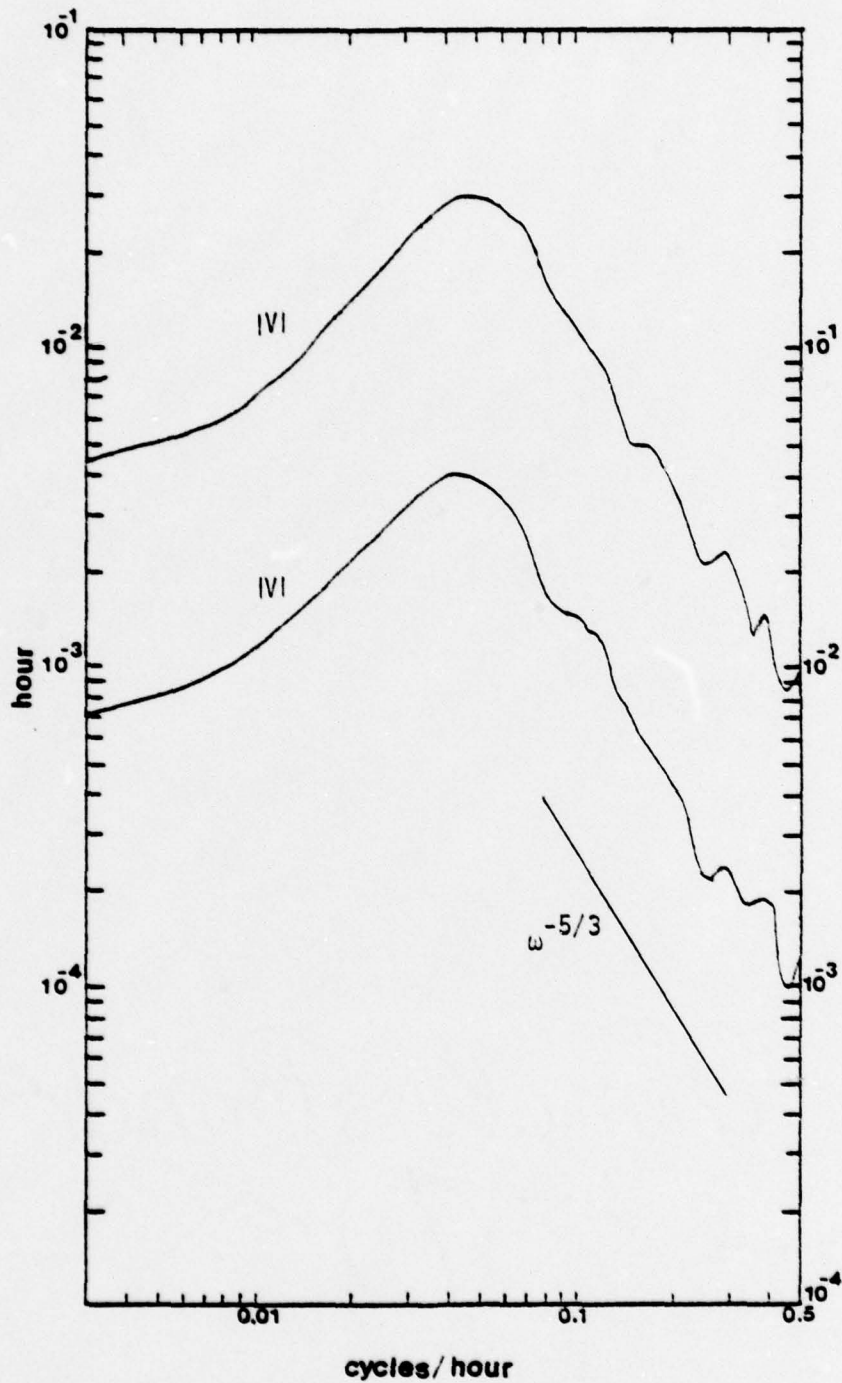


Figure 15. Normalized spectral density of the wind speed for suburban St. Louis under stable conditions (top) and neutral (bottom).

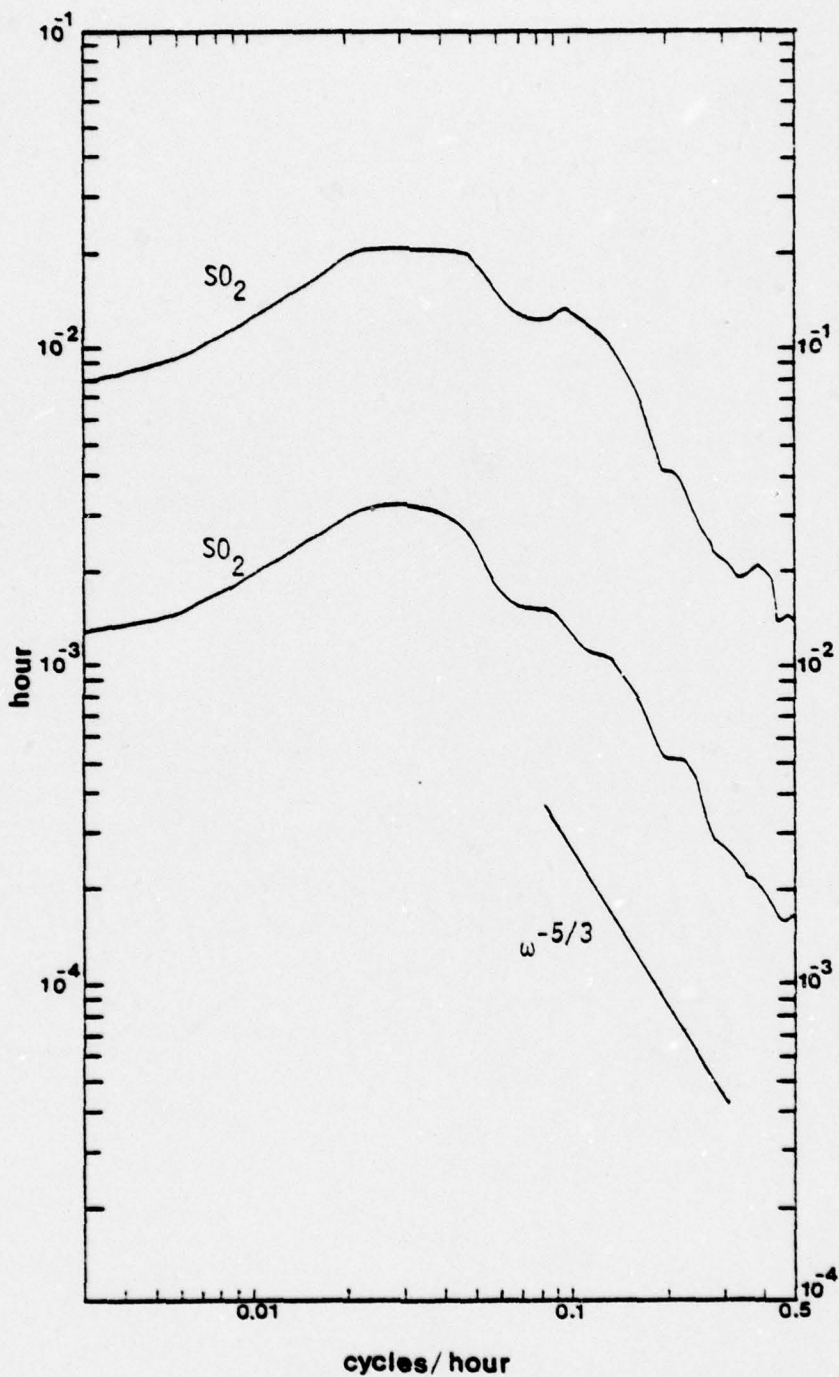


Figure 16. Normalized spectral density of the SO₂ for suburban St. Louis under stable conditions (top) and neutral (bottom).

does appear in the urban neutral SO_2 spectrum, (Figure 14).

From the above analysis it seems that forecasting the SO_2 spectrum from the wind spectrum for the stable category can be successful for the 0.02 to 0.05 and 0.08 to 0.10 cycles/hour ranges (24 and 12 hour periods) and possibly for the 8 hour period and 0.003 to 0.015 cycles/hour ranges. The ability to forecast the SO_2 spectra for neutral and unstable categories is doubtful.

The Inertial Sub-range

The energy decrease in the spectrum provides information about the mechanisms affecting the distribution of energy under various stability conditions. Pasquill (1962) stated that convectively induced turbulence in the inertial sub-range will cause energy to decrease with increasing frequency and the spectral density at frequency n takes the form of

$$F(n) \propto \epsilon^{2/3} n^{-5/3} \quad (25)$$

where ϵ is rate of energy dissipation per unit mass of fluid. So as n increases in the inertial sub-range where convectively induced turbulence occurs, $F(n)$ will decrease at a rate proportional to $n^{-5/3}$. Thus, Pasquill's equation is named the "minus 5/3 power law". This means the decreasing portion of each spectrum should have a slope of $-5/3$. Pasquill also stated that convectively induced turbulence extends the region in which energy decreases rapidly with increasing frequency, and thereby the range over which a "minus 5/3 power law" applies.

To evaluate the accuracy of this theory to the spectral

analysis conducted in this study, a best fit straightline was estimated for the decreasing portion of each spectrum. See Tables 2 and 3 for the results. From Tables 2 and 3, it is obvious that the slope does not obey the minus $5/3$ power law in all cases. However, the inertial sub-range is extended to lower frequencies with increasing instability. This is shown in the table and by observing the respective spectra.

Another result of the wind speed spectra is the increase in the absolute value of the slope with decreasing stability for stations in the Salt Lake area. The likely reason for the change in slope is that under stable conditions the large scale motions are suppressed by the inversion, but the small scale motions are not influenced by the inversion. More energy can remain in the higher frequencies, and have a smaller decreasing absolute slope. Under neutral or unstable conditions, the microscale turbulence is more locally isotropic than under stable conditions, therefore, little constraint to the large scale motion exists and the lower frequency waves absorb more energy. Waves of higher frequencies show relatively less energy, and the spectrum shows a steeper slope.

Kao, Paegle and Normington (1974) found that in the Salt Lake Valley, higher frequencies have a more pronounced contribution to the spectral densities below the mountain tops, particularly close to the surface. Therefore, the slope would be less in the Salt Lake Valley than under equal stability conditions in a flat area such as St. Louis. Since a direct comparison between Salt Lake stations and St. Louis stations cannot be made because of different methods of determining stability category, a firm conclusion cannot be drawn about the

Table 2
The Slope of the Wind Speed Spectra

Station	Stability	Frequency Range (cycles/hour)	Slope
Magna	Stable	0.14 to 0.5	-1.16
	Neutral	0.13 to 0.5	-1.40
	Unstable	0.045 to 0.5	-1.52
Bountiful	Stable	0.18 to 0.28	-1.49
	Neutral	0.175 to 0.275	-1.82
St. Louis-Urban	Stable	0.18 to 0.5	-2.25
Suburban	Stable	0.15 to 0.5	-1.95
Urban	Neutral	0.08 to 0.5	-1.63
Suburban	Neutral	0.10 to 0.5	-1.66

Table 3
The Slope of the SO₂ Spectra

Station	Stability	Frequency Range (cycles/hour)	Slope	
Magna	Stable	0.04 to 0.13	-1.20	
		0.13 to 0.50	-1.66	
	Neutral	0.04 to 0.10	-0.92	
		0.10 to 0.50	-1.44	
	Unstable	0.04 to 0.09	-1.94	
		0.09 to 0.20	-0.37	
		0.20 to 0.50	-1.43	
Kearns	Stable	0.05 to 0.15	-0.75	
		0.15 to 0.50	-1.74	
Tooele	Stable	0.05 to 0.15	-0.93	
		0.15 to 0.50	-1.95	
Bountiful	Stable	0.175 to 0.50	-1.73	
	Neutral	0.125 to 0.50	-1.73	
St. Louis-Urban	Stable	0.12 to 0.50	-1.62	
		Suburban	0.16 to 0.50	-1.71
	Urban	Neutral	0.10 to 0.50	-1.42
	Suburban		0.13 to 0.50	-1.55

"mountain effect" that Kao, Paegle and Normington (1974) found. But their findings might explain why the slope at Magna during stable periods was -1.16 and at St. Louis -2.25 for urban and -1.95 for suburbs in stable periods. The neutral spectra for the same locations show a slope of -1.40 and at St. Louis about -1.65 for urban and suburban stations.

The slope in the inertial sub-range of the SO_2 spectra for all sites decreases with decreasing stability. Also, the decrease is broken into two or three slopes in the Magna spectra. The difference in the SO_2 and wind speed decrease can be partly explained because SO_2 concentrations which are a scalar quantity, are dependent on the wind.

Lake/River Effect

The 12 hour period in the wind speed in the Salt Lake Valley due to the lake-land circulation was confirmed by Kao, Lee and Smidy (1975). In this study, the 12 hour period appears, but with varying degrees depending on stability. From Figure 17, one can see the decrease in amplitude of the 12 hour period from stable through unstable categories. In the SO_2 spectra, a prominent 12 hour peak occurs only in the stable category (Figure 18).

A river effect is found in the data obtained at St. Louis, but to a much smaller degree than the Great Salt Lake effect in the Salt Lake Valley as shown in Figures 13, 14, 15, 16, 17, and 18. For stable periods, the 12 hour period set up in the St. Louis area appears between 0.095 to 0.12 cycles/hour in the wind speed spectra. In stable periods the SO_2 spectrum for the urban stations shows a greater amplitude in the frequencies near 0.083 cycles/hour (12 hour periods) than the sub-

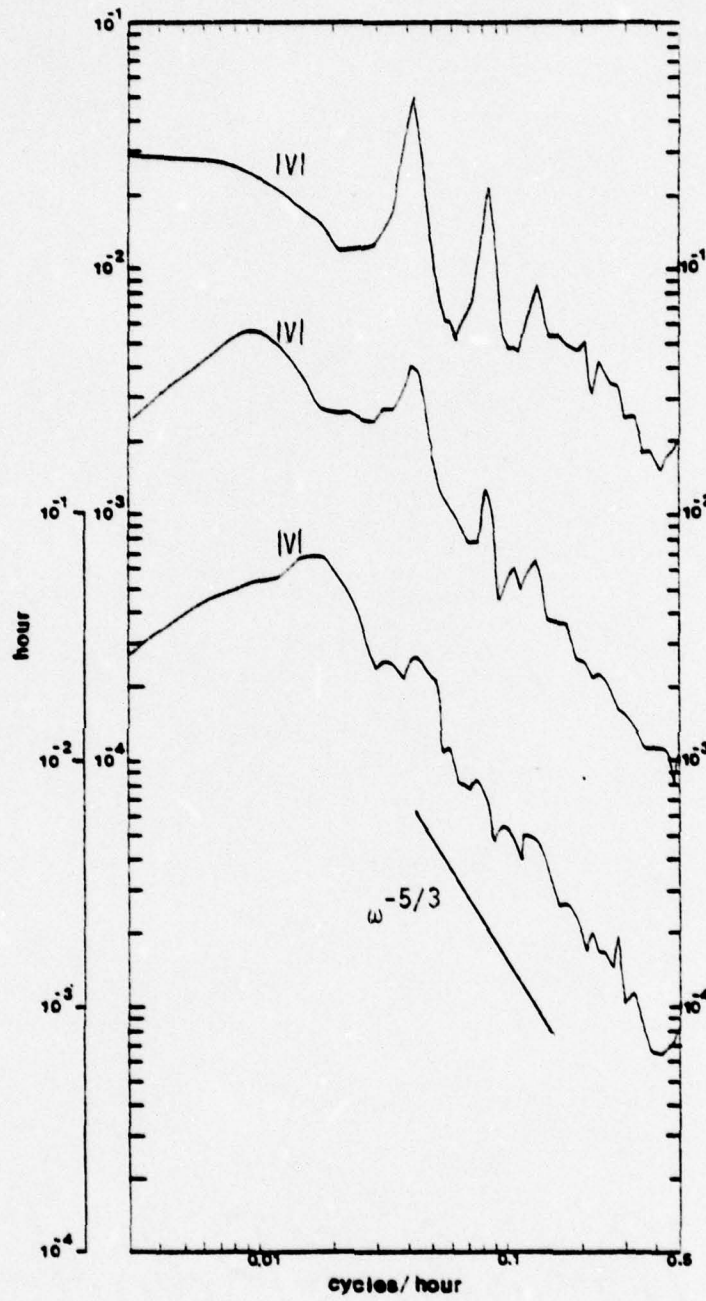


Figure 17. Normalized spectral density of the wind speed at Magna under stable conditions (top), neutral (middle) and unstable (bottom).

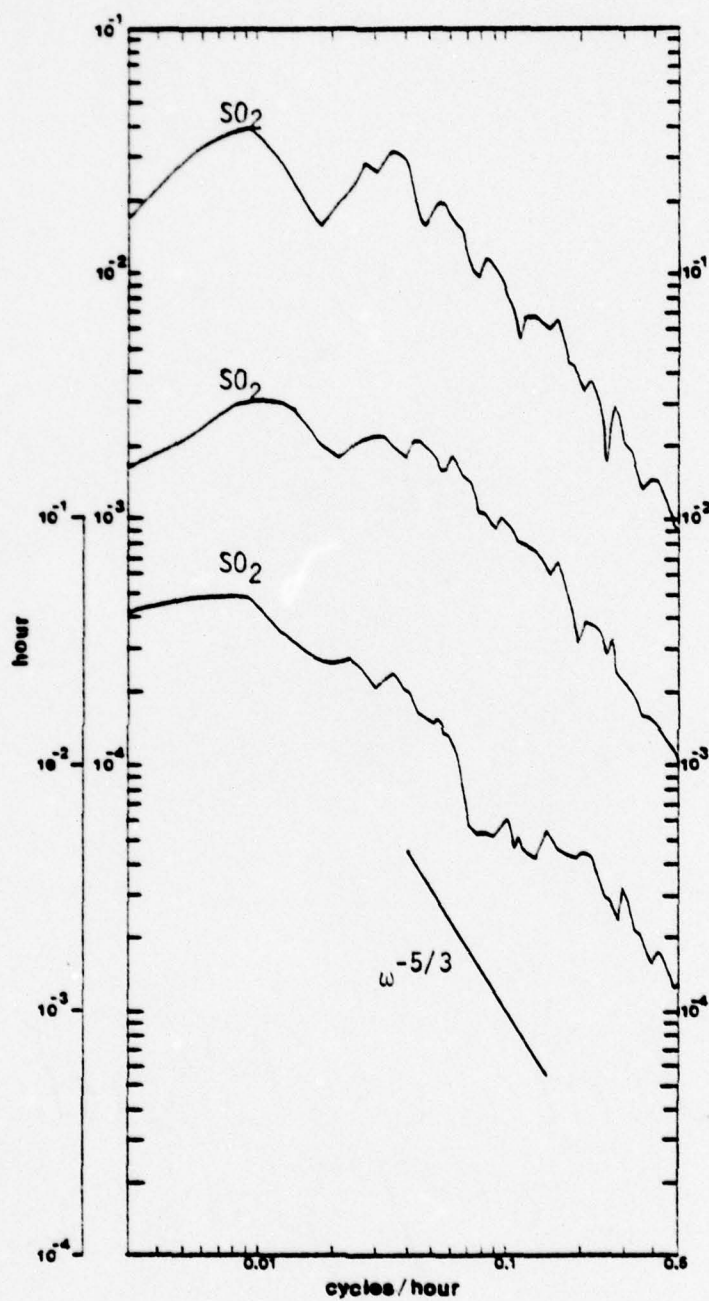


Figure 18. Normalized spectral density of the SO₂ at Magna under stable conditions (top), neutral (middle) and unstable (bottom).

urban stations. The neutral periods for both urban and suburban stations show little energy in the 12 hour period. From the above observations, we can conclude that the river effect does not exist far from the river banks and only appears in stable conditions.

Effects of Local Wind Patterns on the Spectra

Of the four Salt Lake vicinity stations, only two, Magna and Kearns, are in the same valley (Figure 2). The local wind patterns in the different valleys have specific effects on the spectra.

The SO_2 spectra for stable conditions at Magna and Kearns are very similar as shown in Figures 18 and 19, which is expected since both sites are located in the western part of the Salt Lake Valley.

The Tooele SO_2 spectrum under stable conditions as shown in Figure 20, shows one marked difference compared to spectra at Magna and Kearns. The difference is the 24 hour peak. Tooele's 24 hour peak is much larger than Magna or Kearns peak indicating a difference in the type of diffusion in the Tooele Valley compared to the Salt Lake Valley. The Salt Lake Valley is closed to the south by a mountain boundary whereas the Tooele Valley is open to the north and south. A tunneling effect is set up and enhances the lake-valley circulation.

The spectra at Bountiful as shown in Figures 21 and 22, differs considerably from any of the other Salt Lake vicinity stations in two ways: first, the highest peak in the stable wind speed spectrum is 12, not 24 hours; second, much more energy is contained in the higher frequencies of the wind speed spectra at Bountiful under both the stable and neutral conditions.

The two differences are attributed to the lake breeze coupled

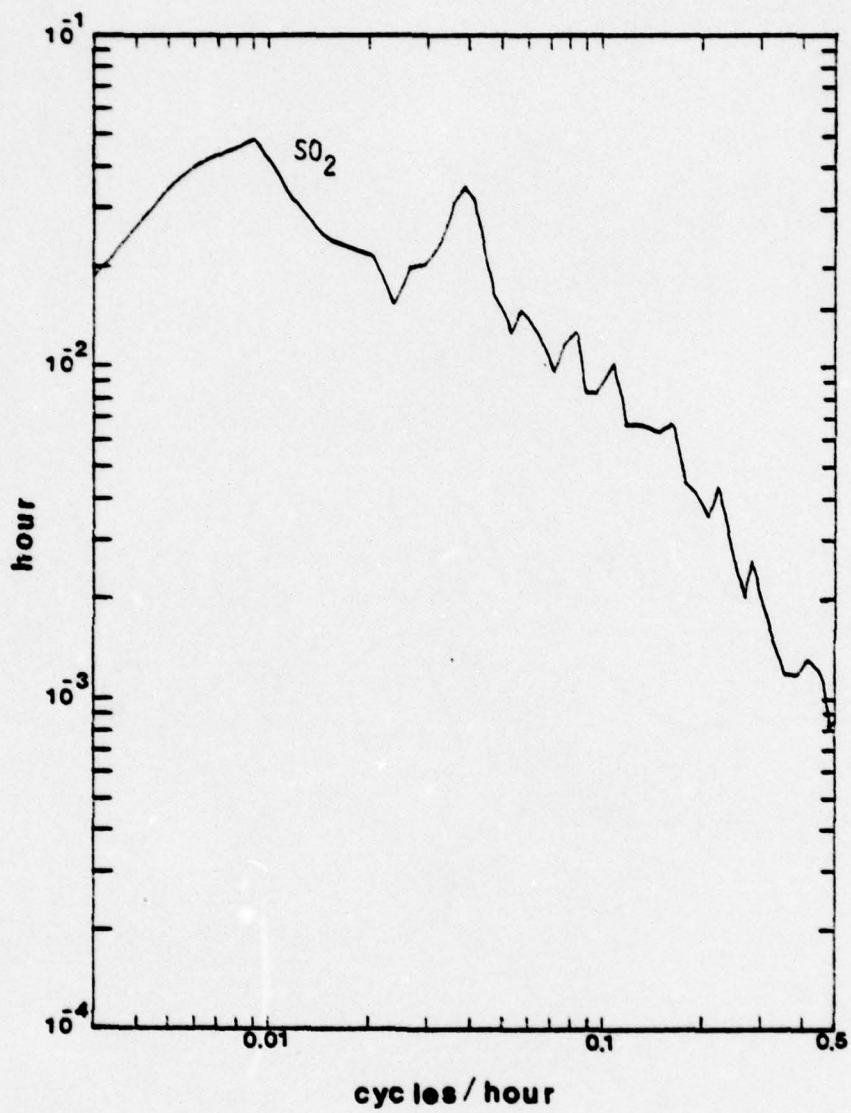


Figure 19. Normalized spectral density of the SO₂ at Kearns under stable conditions.

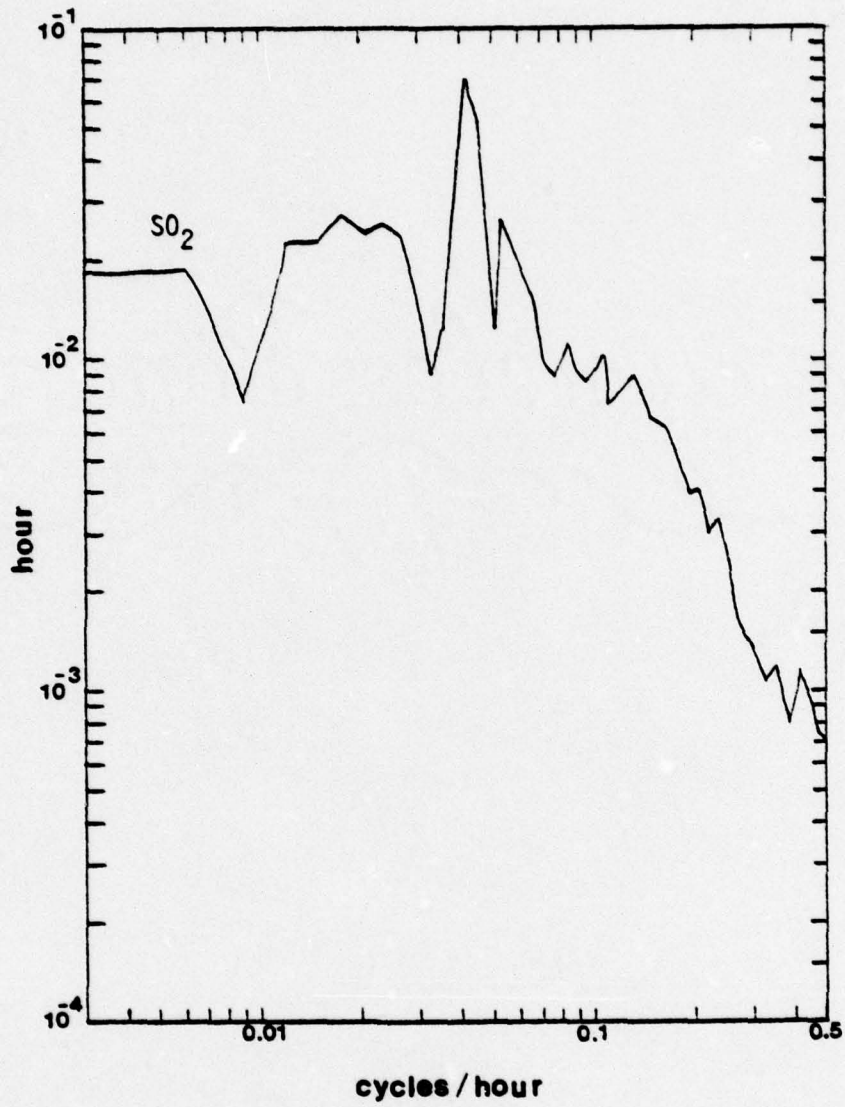


Figure 20. Normalized spectral density of the SO₂ at Tooele under stable conditions.

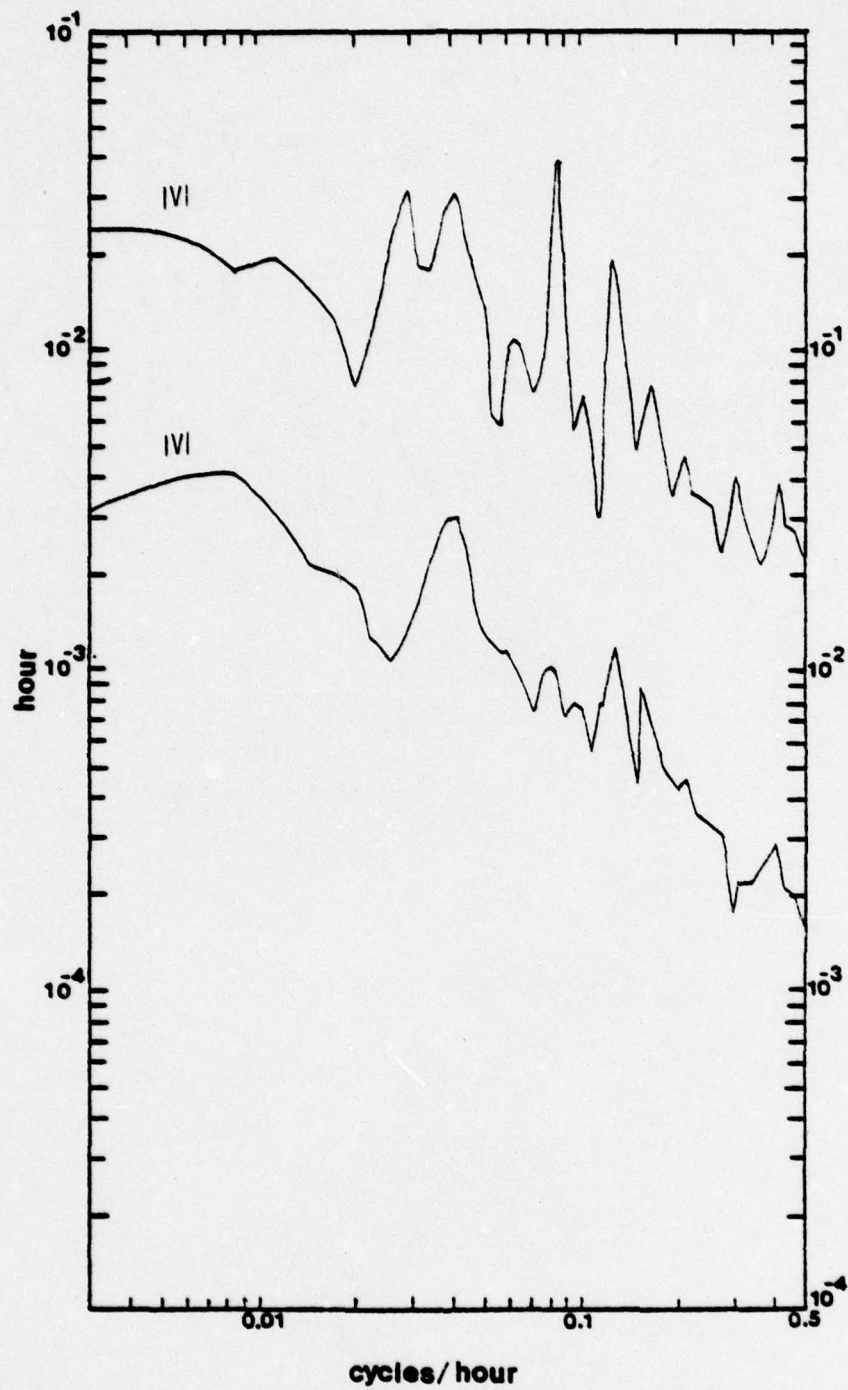


Figure 21. Normalized spectral density of the wind speed at Bountiful under stable conditions (top) and neutral (bottom).

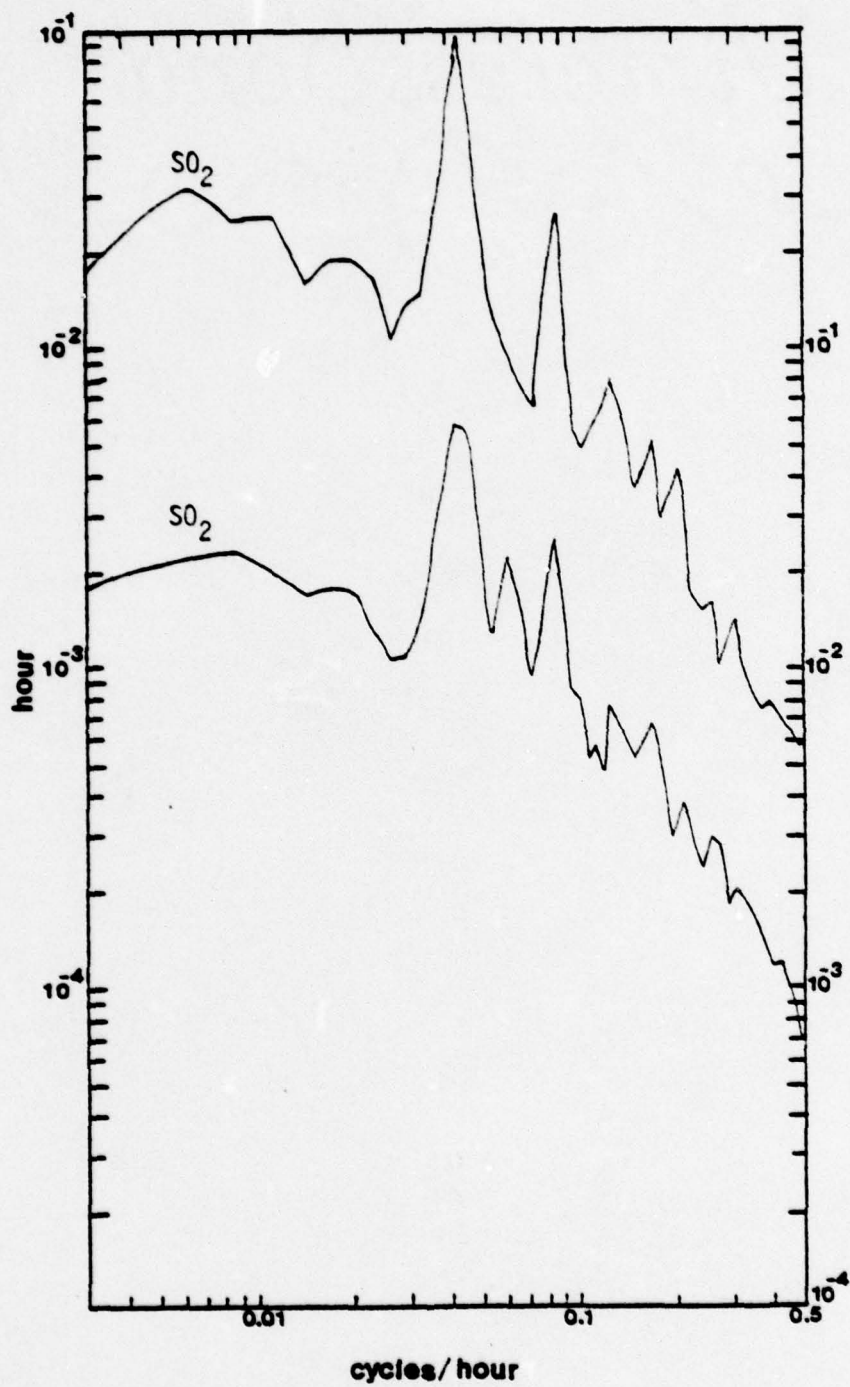


Figure 22. Normalized spectral density of the SO₂ at Bountiful under stable conditions (top) and neutral (bottom).

with canyon winds. Several deep canyons are located in the Wasatch Mountain Range just to the east-south-east (ESE) of Bountiful and the Great Salt Lake is several miles to the west (Figure 2). Between the hours of 10:00 p.m. and 9:00 a.m., the prevailing winds are ESE out of the canyons at Bountiful compared to the prevailing winds at Magna out of the south-south-west (Figures 23 and 24). With a lake/canyon wind regime, the 12 hour peak is explained.

The additional energy in the higher frequencies of the Bountiful wind spectra (Figure 21) is caused by an increase of energy in turbulent eddies due to the canyon winds. Significant energy appears in the periods ranging from 3.5 to 2 hours. At this frequency range, aliasing has probably occurred and indicates considerable energy is in frequencies higher than 0.5 cycles/hour. The relatively large amount of energy in the higher frequencies indicates that even under stable conditions, canyon winds produce high amounts of turbulence.

The canyon winds do not affect the SO_2 spectra in the higher frequencies, but the lake-canyon wind shift does develop a very prominent 12 and 24 hour peak.

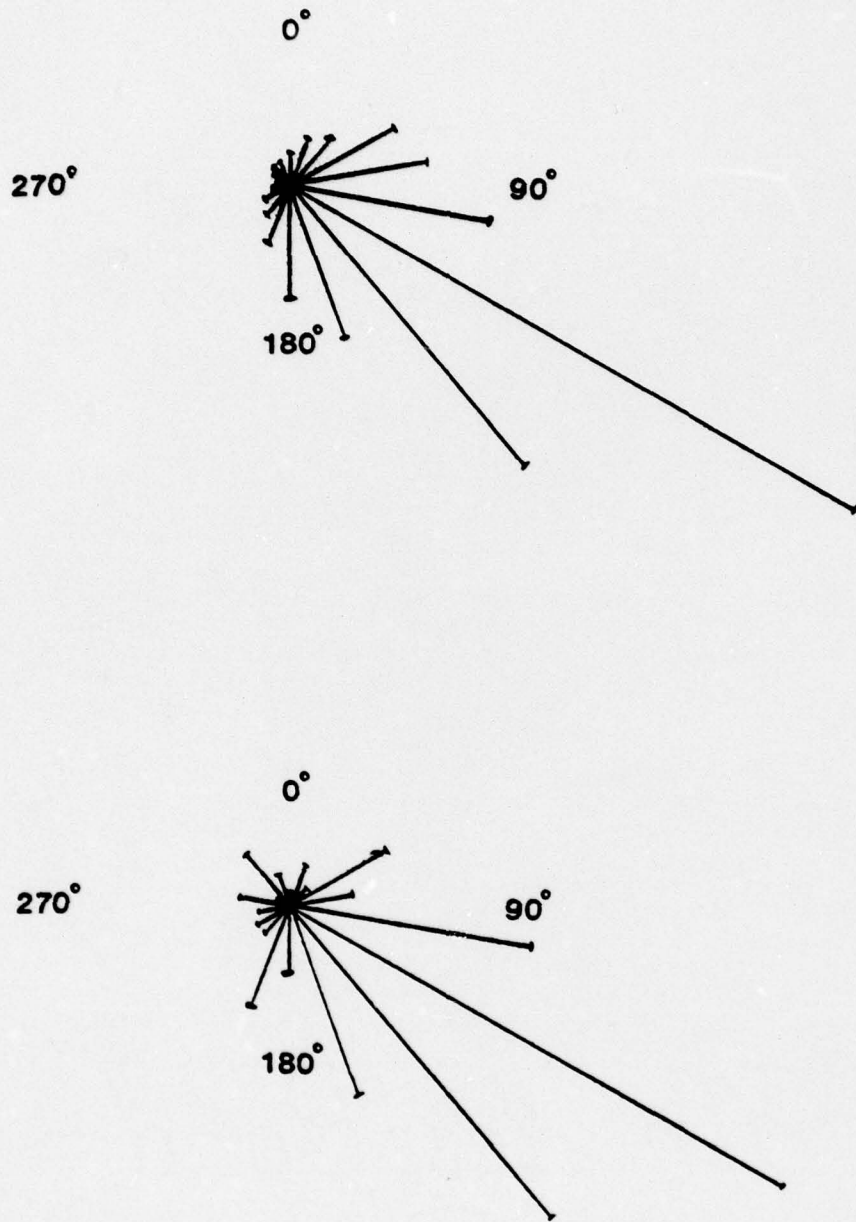


Figure 23. Wind rose of Bountiful under stable conditions (top) and neutral (bottom).

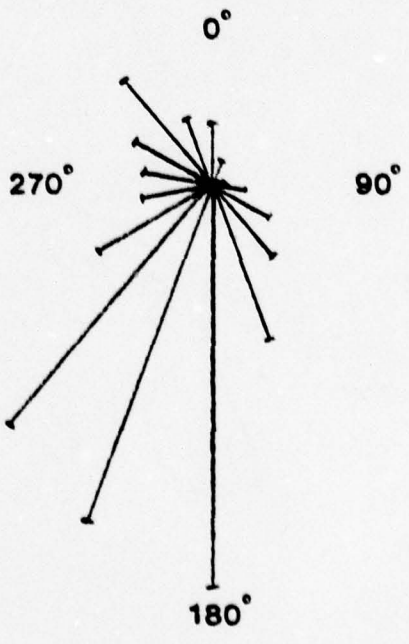
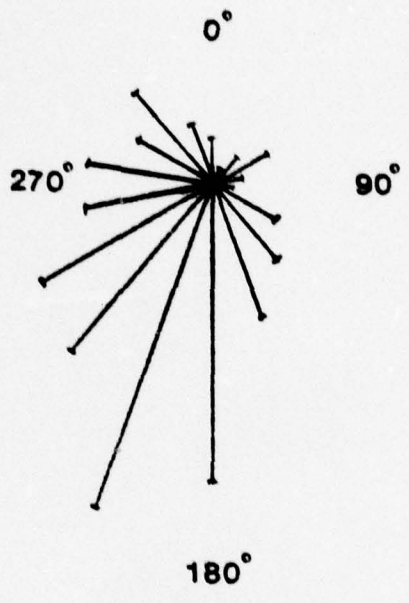


Figure 24. Wind rose of Magna under stable conditions (top) and neutral (bottom).

CHAPTER 7

SUMMARY

Regarding auto- and cross-correlograms it is found from this study:

1. The similarity decreases between wind speed and SO_2 auto-correlograms with decreasing stability.

2. The first zero autocorrelation coefficient occurs near the time lag of four to five hours for both wind speed and SO_2 .

3. The 24 hour moving average gives the best similarity in the auto-correlograms of the hour averaged data among stability categories for both wind speed and SO_2 .

4. If only the linear trend is eliminated, then the differences in the integral areas among stability categories will be larger.

5. For stable periods the time lag of one hour has the highest correlation in the cross-correlogram of SO_2 for Magna vs. Kearns.

The following results were found from spectral analysis:

1. The Magna wind speed spectrum greatly affects the SO_2 spectrum for periods equal to or less than 24 hours under stable conditions.

2. Under stable conditions for periods longer than 24 hours the SO_2 spectrum is probably more influenced by the buildup of SO_2 trapped in the Salt Lake Valley than by the wind speed spectrum.

3. The similarity between the spectra of wind speed and SO_2

decreases with decreasing stability.

4. Forecasting the SO_2 spectrum from the wind speed spectrum for stable periods is possible for the ranges of 0.02 to 0.05 and 0.08 to 0.10 cycles/hour.

5. For both wind speed and SO_2 spectra the range over which the energy decreases is extended to lower frequencies with decreasing stability.

6. In stable periods the large scale motions are suppressed by the inversion, but the small scale motions are free to absorb energy. In unstable periods little constraint on the large scale motion exists and the lower frequency waves absorb more energy.

7. The slope of the energy decrease at Magna for the wind speed spectrum is less than at St. Louis in stable periods probably because in mountainous terrain the higher frequencies have more contribution to the total energy than in flat terrain.

8. The lake effect in the Salt Lake vicinity produces a 12 hour peak in the wind speed spectra. To a lesser degree the Mississippi River produces a river effect close to the river banks, but only in stable periods.

9. The local wind patterns in the different Salt Lake vicinity valleys have specific effects on the spectra.

APPENDIX A

AUTO- AND CROSSCORRELATION PROGRAMS

The first program calculates the autocorrelation coefficients at one station, and the second program calculates the crosscorrelation coefficients between two stations. Both eliminate the linear trend using the subroutine Linear Trend Removal used in the first program of Appendix B. When correlations using a 24 hour moving average are desired, replace the Linear Trend Removal subroutine with Equation (18) of Chapter 3. All programs in Appendix A and B are written by the author, and ICASE is the number of realizations for each case and M is the length of the respective realization.

```

C PROGRAM TO CALCULATE THE AUTOCORRELATION COEFFICIENTS FOR
C ONE STATION AND ONE STABILITY CONDITION
  DIMENSION A(336), XPRIME(336), RTAU(29,48), XPRIS2(29,48),
  =TRTAU(48), TXPRIS(48)
  ICASE = 16
  KI = 1
1  DO 9 K=1, ICASE
    IF (K .LE. 4) GO TO 101
    IF (K .LE. 6) GO TO 102
    IF (K .LE. 10) GO TO 103
    IF (K .LE. 13) GO TO 104
    IF (K .EG. 14) GO TO 105
    IF (K .EG. 15) GO TO 106
    IF (K .EG. 16) GO TO 107
101 M= 96
    GO TO 200
102 M= 120
    GO TO 200
103 M= 144
    GO TO 200
104 M= 168
    GO TO 200
105 M= 192
    GO TO 200
106 M= 240
    GO TO 200
107 M= 336
200 CONTINUE
    DO 10 I= 1, M, 12
      READ (5,501) A(I), A(I+1), A(I+2), A(I+3), A(I+4), A(I+5), A(I+6),
      =A(I+7), A(I+8), A(I+9), A(I+10), A(I+11)
10  CONTINUE
501 FORMAT (12F5.2)
      MM12= M - 12
      MM13= M - 13
      CALL LTR (M, A, AV)
      DO 13 L= 13, MM12
13  XPRIME(L) = A(L)
C CALCULATE THE AUTOCORRELATION COEFFICIENTS USING THE
C BOX AND JENKINS METHOD
      DO 15 I= 1, 48
        XPRISM= 0.
        XBOXJK= 0.
        RTAU(K, I)= 0.
        XPRIS2(K, I)= 0.
        DO 16 L= 13, MM13
          AUTOCC = XPRIME(L) * XPRIME(L+I)
          XPRISG = XPRIME(L)**2.
          XPRILG = XPRIME(L+I)**2.
          RTAU(K, I) = AUTOCC + RTAU(K, I)
          XPRISM = XPRISG + XPRISM
          XBOXJK = XPRILG + XBOXJK
16  XPRIS2(K, I) = (XPRISM+XBOXJK)**0.5
          RXE = RTAU(K, I)/XPRIS2(K, I)
15  MM13= MM13 - 1
9  CONTINUE
      WRITE (6,620)
620 FORMAT (//10X, 'TOTAL AUTOCORRELATIONS FOR ONE CLASS OF CLEARING
      . INDEX //)

```

THIS PAGE IS BEST QUALITY PRACTICABLE
FROM COPY FURNISHED TO DDC

62

```
DO 20 I= 1,48
  TRTAU(I)= 0.
  TXPRIS(I)= 0.
  DO 21 K= 1,ICASE
    TRTAU(I) = TRTAU(I) + RTAU(K,I)
  21 TXPRIS(I) = TXPRIS(I) + XPRIS2(K,I)
    TOTRXE = TRTAU(I)/TXPRIS(I)
  WRITE (6,621) I, TOTRXE, TRTAU(I), TXPRIS(I)
621 FORMAT (10X,'TAU=',I3,5X,'TOTRXE=',F10.7,5X,'TRTAU=',E12.7,5X,
  *TXPRIS=',E12.7)
  20 CONTINUE
    KI= KI +1
    IF (KI .EQ. 2) GO TO 1
  STOP
  END
```

THIS PAGE IS BEST QUALITY PRACTICABLE
FROM COPY FURNISHED TO DDC

```

C PROGRAM TO CALCULATE CROSSCORRELATION COEFFECIENTS BETWEEN ANY
C TWO STATIONS
  DIMENSION A(336),XPRIME(336),RTAU(29,48),XPRIS2(29,48),
  *TRTAU(48), TXPRIS(48),B(336),BPRIME(336),
  *CRTAU(29,48),TCTAU(48),TCPRI(48),CPRIS2(29,48),
  *RZERCO(29), RZERSG(29), RZERLG(29)
  ICASE = 16
  DO 9 K=1,ICASE
  IF (K .LE. 4) GO TO 101
  IF (K .LE. 6) GO TO 102
  IF (K .LE. 10) GO TO 103
  IF (K .LE. 13) GO TO 104
  IF (K .EQ. 14) GO TO 105
  IF (K .EQ. 15) GO TO 106
  IF (K .EQ. 16) GO TO 107
101 M= 96
  GO TO 200
102 M= 120
  GO TO 200
103 M= 144
  GO TO 200
104 M= 168
  GO TO 200
105 M= 192
  GO TO 200
106 M= 240
  GO TO 200
107 M= 336
200 CONTINUE
  DO 10 I= 1,M,12
  READ (5,501) A(I), A(I+1), A(I+2), A(I+3), A(I+4), A(I+5), A(I+6),
  *A(I+7), A(I+8), A(I+9), A(I+10), A(I+11)
  10 CONTINUE
501 FORMAT (12F5,2)
  DO 50 I= 1,M,12
  READ (5,501) B(I),B(I+1),B(I+2),B(I+3),B(I+4),B(I+5),B(I+6),
  *B(I+7),B(I+8),B(I+9),B(I+10),B(I+11)
  50 CONTINUE
  MM12= M - 12
  MM13= M - 13
  CALL LTR (M,A,AV)
  CALL LTR (M,B,AV)
  DO 13 L= 13,MM12
  BPRIME(L) = B(L)
  13 XPRIME(L) = A(L)
  RZERCO(K)= 0.
  RZERSG(K)= 0.
  RZERLG(K)= 0.
  DO 17 L= 13,MM12
  ZEROCO = XPRIME(L)*BPRIME(L)
  ZEROSG = XPRIME(L)**2.
  ZEROLG = BPRIME(L)**2.
  RZERCO(K) = ZEROCO + RZERCO(K)
  RZERSG(K) = ZEROSG + RZERSG(K)
  17 RZERLG(K) = ZEROLG + RZERLG(K)
  DO 15 I= 1,48
  XPRISM= 0.
  XBOXJK= 0.
  RTAU(K,I)= 0.
  XPRIS2(K,I)= 0.

```

```
CPRISM = 0.  
CBOXJK = 0.  
CRTAU(K,I) = 0.  
CPRIS2(K,I) = 0.  
DO 16 L= 13,MM13  
AUTOCO = XPRIME(L) * BPRIME(L+I)  
CNEGCO = BPRIME(L)*XPRIME(L+I)  
XPRISQ = XPRIME(L)**2.  
XPRILG = BPRIME(L+I)**2.  
CNEGSQ = BPRIME(L)**2.  
CNEGLG = XPRIME(L+I)**2.  
XPRISM = XPRISQ + XPRISM  
XBOXJK = XPRILG + XBOXJK  
CPRISM = CNEGSQ + CPRISM  
CBOXJK = CNEGLG + CBOXJK  
RTAU(K,I) = AUTOCO + RTAU(K,I)  
16 CRTAU(K,I) = CNEGCO + CRTAU(K,I)  
XPRIS2(K,I) = (XPRISM*XBOXJK)**0.5  
CPRIS2(K,I) = (CPRISM*CBOXJK)**0.5  
15 MM13= MM13 - 1  
9 CONTINUE  
TZERCO = 0.  
TZERSQ = 0.  
TZERLG = 0.  
DO 22 K= 1,ICASE  
TZERCO = RZERCO(K) + TZERCO  
TZERSQ = RZERSQ(K) + TZERSQ  
22 TZERLG = RZERLG(K) + TZERLG  
TOTZC1 = TZERCO/TZERSQ  
TOTZC2 = TZERCO/TZERLG  
TOTZC3 = TZERCO/(TZERSQ*TZERLG)**0.5  
WRITE (6,622) TOTZC1, TOTZC2, TOTZC3  
622 FORMAT (10X,'TOTZC1=',F7.4,5X,'TOTZC2=',F7.4,5X,'TOTZC3=',F7.4//)  
WRITE (6,620)  
620 FORMAT(//10X,'TOTAL AUTOCORRELATIONS FOR ONE CLASS OF CLEARING  
= INDEA'//)  
DO 20 I= 1,48  
TRTAU(I)= 0.  
TXPRIS(I)= 0.  
TCTAU(I) = 0.  
TCPRIS(I) = 0.  
DO 21 K= 1,ICASE  
TRTAU(I) = TRTAU(I) + RTAU(K,I)  
TXPRIS(I) = TXPRIS(I) + XPRIS2(K,I)  
TCTAU(I) = TCTAU(I) + CRTAU(K,I)  
21 TCPRIS(I) = TCPRIS(I) + CPRIS2(K,I)  
TOTRXE = TRTAU(I)/TXPRIS(I)  
TOTCXE = TCTAU(I)/TCPRIS(I)  
WRITE (6,621) I, TOTRXE, TRTAU(I), TXPRIS(I), TOTCXE,  
TCTAU(I), TCPRIS(I)  
621 FORMAT ('TAU=',I3,3X,'TOTRXE=',F7.4,3X,'TRTAU=',E9.4,1X,'TXPRIS=',  
E9.4,1X,'TOTCXE=',F7.4,3X,'TCTAU=',E9.4,1X,'TCPRIS=',E9.4)  
20 CONTINUE  
STOP  
END
```

APPENDIX B

SPECTRAL DENSITY PROGRAMS

The spectral densities are calculated for the Salt Lake Valley and vicinity stations in the first program and for the St. Louis urban and suburban stations in the second program. The two subroutines, Linear Trend Removal and Cosine Bell Window, are modified in the first program so that the 12 first and last data points are not used. This step is necessary since 12 extra data points were added to the Salt Lake Valley and vicinity data so that in the programs of Appendix A the \bar{u}_1 and the \bar{u}_N of the 24 hour moving average could be calculated.

```
C PROGRAM FOR CALCULATING THE POWER SPECTRUM FROM A SINGLE MONITOR
C FOR MANY POLLUTION CASES USING THE DIRECT TRANSFORM METHOD ON PAGE
C 82 - 83 RAYNER (1971) AND MODIFIED SUBROUTINES FROM LEE AND HATCH.
  DIMENSION A(336),C(168),IWK(1049),E(336),XPRIME(336),
  *CVAR(29), CSPEC(29,169),SPEC(29,169),XVAR(29),TSPEC(169),
  *TCSPEC(169), SPAV6(169)
  COMPLEX C, GAMN
  EQUIVALENCE (E,C)
  N= 336
  N2 = N/2
  N3 = N2 + 1
  P= 0.1
  ICASE= 18
  KI= 1
  1 DO 9 K=1, ICASE
    IF (K .LE. 6) GO TO 101
    IF (K .LE. 10) GO TO 102
    IF (K .LE. 11) GO TO 103
    IF (K .LE. 14) GO TO 106
    IF (K .LE. 17) GO TO 110
    IF (K .EQ. 18) GO TO 107
  101 M= 96
    GO TO 200
  102 M= 120
    GO TO 200
  103 M= 144
    GO TO 200
  106 M= 216
    GO TO 200
  110 M = 240
    GO TO 200
  107 M= 336
  200 CONTINUE
    IZ = (N-M)/2 + 12
    MM12 = M - 12
    MM24 = M - 24
    M24IZ1 = M - 24 + IZ + 1
    DO 10 I= 1,M,12
      READ (5,501) A(I), A(I+1), A(I+2), A(I+3), A(I+4), A(I+5), A(I+6),
      *A(I+7), A(I+8), A(I+9), A(I+10), A(I+11)
  501 FORMAT (12F5.2)
    10 CONTINUE
      CALL LTR(M,A,AVG)
      CALL WINDOW (M,A,P)
C GIVE ALL THE PERIODS THE SAME LENGTH BY ADDING EQUAL NUMBER OF
C ZEROS TO BOTH ENDS OF THE DATA.
    DO 53 I= 1,IZ
      53 XPRIME(I)= 0.
    DO 52 I= 1,MM24
      52 XPRIME(I+IZ) = A(I+12)
    DO 54 I= M24IZ1,N
      54 XPRIME(I)= 0.
C CALCULATE THE SPECTRUM USING THE FAST FOURIER TRANSFORM ALGORITHMN.
    DO 45 KK= 1,N
      45 E(KK) = XPRIME(KK)
      CALL FFTR(E,GAMN,N,IWK)
      DO 30 KK= 1,N2
        30 C(KK) = C(KK)/FLOAT(N2)
          GAMN= GAMN/FLOAT(N2)
```

```

DO 35 I= 1,N2
35 SPEC(K,I) = CABS(C(I))**2./2.
   SPEC(K,N3) = CABS(GAMN)**2.
   CVAR(K) = 0.
   DO 50 I= 1,N2
50 CVAR(K) = SPEC(K,I) + CVAR(K)
   CVAR(K) = CVAR(K) + SPEC(K,N3)
   DO 21 I= 1,N3
21 CSPEC(K,I) = SPEC(K,I)/CVAR(K)
   Y= 0.
   DO 70 I= 1,N
70 Y= Y + XPRIME(I)**2.
   XVAR(K) = Y/N
9 CONTINUE
C ENSEMBLE AVERAGE THE CASES FOR EACH STABILITY CLASS.
   TCVAR = 0.
   TXVAR = 0.
   DO 22 K= 1,ICASE
   TCVAR = CVAR(K) + TCVAR
22 TXVAR = XVAR(K) + TXVAR
   DO 23 I= 1,N3
   TCSPEC(I) = 0.
   TSPEC(I) = 0.
   DO 24 K= 1,ICASE
   TSPEC(I) = SPEC(K,I) + TSPEC(I)
24 TCSPEC(I) = CSPEC(K,I) + TCSPEC(I)
23 CONTINUE
   DO 25 I= 1,N3
   TSPEC(I) = TSPEC(I)/(ICASE*TCVAR)
25 TCSPEC(I) = TCSPEC(I)/ICASE
C AVERAGE THE POWER SPECTRA IN THE HIGHER FREQUENCIES, (0.065
C CYCLES/HOUR AND HIGHER).
   DO 27 I= 22,40,2
27 SPAVG(I+1) = (TCSPEC(I) + TCSPEC(I+1))/2.
   DO 28 I= 42,97,5
28 SPAVG(I+4) = (TCSPEC(I) + TCSPEC(I+1) + TCSPEC(I+2) + TCSPEC(I+3)
* + TCSPEC(I+4))/5.
   DO 29 I= 102,152,10
29 SPAVG(I+9) = (TCSPEC(I) + TCSPEC(I+1) + TCSPEC(I+2) +
* TCSPEC(I+3) + TCSPEC(I+4) + TCSPEC(I+5) + TCSPEC(I+6) +
* TCSPEC(I+7) + TCSPEC(I+8) + TCSPEC(I+9))/10.
   DO 31 I= 162,168
31 SPAVG(168) = SPAVG(168) + TCSPEC(I)
   SPAVG(168) = SPAVG(168)/7.
WRITE(6,610)
610 FORMAT (/10X,'WAVE',8X,'FREQ',8X,'HOURS',9X,'DAYS',7X,'SPECTRUM',
*9X,'C-SPEC',9X,'SLOPE'/)
   IM0= 0
   WRITE (6,612) IM0, TSPEC(1), TCSPEC(1)
612 FORMAT (10X,I4,42X,E10.5,5X,E10.5)
   DO 26 I= 2,N3
   IM1= I - 1
   HRS= FLOAT(N)/FLOAT(IM1)
   DAYS = HRS/24.
   FREQ = 1./HRS
   WRITE (6,611) IM1,FREQ,HRS,DAYS,TSPEC(I),TCSPEC(I),SPAVG(I)
611 FORMAT (10X,I4,5X,F8.5,5X,F9.2,5X,F8.2,5X,E10.5,5X,E10.5,5X,E10.5)
26 CONTINUE
   WRITE (6,621)TXVAR, TCVAR
621 FORMAT (/10X,'VARIANCE',2X,E10.5,5X,'SPEC VARIANCE',2X,E10.5////)
   KI = KI + 1
   IF (KI .EQ. 2) GO TO 1
STOP
END

```

```
C==== LINEAR TREND REMOVAL PROGRAM
SUBROUTINE LTR(N,X,SX)
DIMENSION X(N)
FN=N-24
MM12=N-12
SX=0.
SP=0.
DO 11 I=13,MM12
11 SX=SX+X(I)
SX=SX/FN
DO 13 I=13,MM12
X(I)=X(I)-SX
13 SP=SP+X(I)*FLOAT(I)
AVI=(FN+1.)/2.
ANG=-12.*SP/(FN*(FN+2-1))
DO 15 I=13,MM12
FI=I
15 X(I)=X(I)-ANG*(AVI-FI)
RETURN
END
```

```
C==== COSINE BELL WINDOW
SUBROUTINE WINDOW(N,X,P)
DIMENSION X(N)
G=P+12.
NTENTH=G
PIG=3.14159265/(G-12.)
NP=N-1
DO 2 I=13,NTENTH
FI=I-12
JNP=NP-I
COSBEL=0.5*(1.-COS(FI*PIG))
X(I)=X(I)*COSBEL
2 X(JNP)=X(JNP)*COSBEL
RETURN
END
```

```
C PROGRAM FOR CALCULATING SPECTRAL DENSITIES FROM SEVERAL MONITORS
C FOR MANY POLLUTION CASES USING THE DIRECT TRANSFORM METHOD ON PAGE
C 82 - 83 RAYNER (1971) AND SUBROUTINES FROM LEE AND HATCH.
  DIMENSION A(336),C(168),IWK(1049),E(336),XPRIME(336),
  *CVAR(29),CSPEC(29,169),SPEC(29,169),XVAR(29),TSPEC(169),
  *AVG(10),TCSPEC(10,169),SPAVG(10,169),AVSPEC(169),TSPAVG(169)
  COMPLEX C, GAMN
  EQUIVALENCE (E,C)
  N= 336
  N2 = N/2
  N3 = N2 + 1
  P= 0.1
  ICASE= 9
  KI= 1
1 DO 9 K=1,ICASE
  IF (K .EQ. 1) M=36
  IF (K .EQ. 2) M=24
  IF (K .EQ. 3) M=48
  IF (K .EQ. 4) M=48
  IF (K .EQ. 5) M= 60
  IF (K .EQ. 6) M= 36
  IF (K .EQ. 7) M= 24
  IF (K .EQ. 8) M= 24
  IF (K .EQ. 9) M= 24
  IZ = (N-M)/2
  LASTZ= N-IZ+1
  DO 10 I= 1,M,12
  READ (5,501) A(I), A(I+1), A(I+2), A(I+3), A(I+4), A(I+5), A(I+6),
  *A(I+7), A(I+8), A(I+9), A(I+10), A(I+11)
501 FORMAT (12F5.2)
  10 CONTINUE
  CALL LTR(M,A,AVG)
  CALL *INDOW(M,A,P)
C GIVE ALL THE PERIODS THE SAME LENGTH BY ADDING EQUAL NUMBER OF
C ZEROS TO BOTH ENDS OF THE DATA.
  DO 53 I= 1,IZ
  53 XPRIME(I)= 0.
  DO 52 I= 1,M
  52 XPRIME(I+IZ) = A(I)
  DO 54 I= LASTZ,N
  54 XPRIME(I)= 0.
C CALCULATE THE SPECTRUM USING THE FAST FOURIER TRANSFORM ALGORITHMN.
  DO 45 KK= 1,N
  45 E(KK) = XPRIME(KK)
  CALL FFTR(E,GAMN,N,IWK)
  DO 30 KK= 1,N2
  30 C(KK) = C(KK)/FLOAT(N2)
  GAMN= GAMN/FLOAT(N2)
  DO 35 I= 1,N2
  35 SPEC(K,I) = CABS(C(I))*2./2.
  SPEC(K,N3) = CABS(GAMN)*2.
  CVAR(K) = 0.
  DO 50 I= 1,N2
  50 CVAR(K) = SPEC(K,I) + CVAR(K)
  CVAR(K) = CVAR(K) + SPEC(K,N3)
  DO 21 I= 1,N3
  21 CSPEC(K,I) = SPEC(K,I)/CVAR(K)
  Y= 0.
  DO 70 I= 1,N
  70 Y= Y + XPRIME(I)*2.
  XVAR(K) = Y/N
  9 CONTINUE
```

```

C ENSEMBLE AVERAGE THE CASES FOR EACH STABILITY CLASS.
  TCVAR = 0.
  TXVAR = 0.
  DO 22 K= 1, ICASE
    TCVAR = CVAR(K) + TCVAR
  22 TXVAR = XVAR(K) + TXVAR
  DO 23 I= 1, N3
    TSPEC(I) = 0.
  DO 24 K= 1, ICASE
    TSPEC(I) = SPEC(K, I) + TSPEC(I)
  24 TCSPEC(KI, I) = CSPEC(K, I) + TCSPEC(KI, I)
  23 CONTINUE
  DO 25 I= 1, N3
    TSPEC(I) = TSPEC(I)/(ICASE+TCVAR)
  25 TCSPEC(KI, I) = TCSPEC(KI, I)/ICASE
C AVERAGE THE POWER SPECTRA IN THE HIGHER FREQUENCIES, (0.065
C CYCLES/HOUR AND HIGHER).
  DO 27 I= 22, 40, 2
  27 SPAVG(KI, I+1) = (TCSPEC(KI, I) + TCSPEC(KI, I+1))/2.
  DO 28 I= 42, 97, 5
  28 SPAVG(KI, I+4) = (TCSPEC(KI, I) + TCSPEC(KI, I+1) + TCSPEC(KI, I+2) +
    *TCSPEC(KI, I+3) + TCSPEC(KI, I+4))/5.
  DO 29 I= 102, 152, 10
  29 SPAVG(KI, I+9) = (TCSPEC(KI, I) + TCSPEC(KI, I+1) + TCSPEC(KI, I+2) +
    *TCSPEC(KI, I+3) + TCSPEC(KI, I+4) + TCSPEC(KI, I+5) + TCSPEC(KI, I+6) +
    *TCSPEC(KI, I+7) + TCSPEC(KI, I+8) + TCSPEC(KI, I+9))/10.
  DO 31 I= 162, 168
  31 SPAVG(KI, 168) = SPAVG(KI, 168) + TCSPEC(KI, I)
  SPAVG(KI, 168) = SPAVG(KI, 168)/7.
  TAVG = 0.
  DO 61 J= 1, ICASE
  61 TAVG = TAVG + AVG(J)
  WRITE (6, 632) TAVG
  632 FORMAT (10X, F10.5///)
  KI = KI + 1
  IF (KI .LE. 7) GO TO 1
C AVERAGE EACH FREQUENCY OF THE THREE URBAN STATIONS
  DO 62 I= 2, N3
  DO 63 J= 1, 3
    TSPAVG(I) = TSPAVG(I) + SPAVG(J, I)
  63 AVSPEC(I) = AVSPEC(I) + TCSPEC(J, I)
    TSPAVG(I) = TSPAVG(I)/3.
    AVSPEC(I) = AVSPEC(I)/3.
    IM1 = I-1
    FREQ = FLOAT(IM1)/FLOAT(N)
  62 WRITE (6, 633) IM1, FREQ, AVSPEC(I), TSPAVG(I)
C AVERAGE EACH FREQUENCY OF THE FOUR SUBURBAN STATIONS
  DO 72 I= 2, N3
  DO 73 J= 4, 7
    TSPAVG(I) = TSPAVG(I) + SPAVG(J, I)
  73 AVSPEC(I) = AVSPEC(I) + TCSPEC(J, I)
    TSPAVG(I) = TSPAVG(I)/4.
    AVSPEC(I) = AVSPEC(I)/4.
    IM1 = I-1
    FREQ = FLOAT(IM1)/FLOAT(N)
  72 WRITE (6, 633) IM1, FREQ, AVSPEC(I), TSPAVG(I)
  633 FORMAT (10X, I4, F12.5, E15.5, E15.5)
  STOP
  END

```

```
C==== LINEAR TREND REMOVAL PROGRAM
SUBROUTINE LTR(N,X,SX)
DIMENSION X(N)
FN=N
SX=0.
SP=0.
DO 11 I=1,N
11 SX=SX+X(I)
SX=SX/FN
DO 13 I=1,N
X(I)=X(I)-SX
13 SP=SP+X(I)*FLOAT(I)
AVI=(FN+1.)/2.
ANG=-12.*SP/(FN*(FN**2-1))
DO 15 I=1,N
FI=I
15 X(I)=X(I)-ANG*(AVI-FI)
RETURN
END
```

```
C==== COSINE BELL WINDOW
SUBROUTINE WINDOW(N,X,P)
DIMENSION X(N)
G=P*N
NTENTH=G
PIG=3.14159265/G
NP=N+1
DO 2 I=1,NTENTH
FI=I
JNP=NP-I
COSBEL=0.5*(1.-COS(FI*PIG))
X(I)=X(I)*COSBEL
2 X(JNP)=X(JNP)*COSBEL
RETURN
END
```

REFERENCES

- Box, G. E. and G. M. Jenkins, 1970: Time Series Analysis; Forecasting and Control, Holden-Day, San Francisco, 30-32.
- Jackman, Dean N., 1968: A Study of Meteorological Effect on Air Pollution in the Salt Lake Valley. Unpublished M.S. Thesis, University of Utah.
- _____ and W. T. Chapman, 1977: Some Meteorological Aspects of Air Pollution in Utah with Emphasis on the Salt Lake Valley. NOAA Technical Memorandum NWS WR-120, 12-18.
- Kao, S. K., J. N. Paegle and W. E. Normington, 1974: Mountain Effect on the Motion in the Atmosphere's Boundary Layer. Boundary-Layer Meteorology, 7, 501-512.
- _____, H. N. Lee and K. I. Smidy, 1975: An Analysis of the Topographical Effect on Turbulence and Diffusion in the Atmosphere's Boundary Layer. Boundary-Layer Meteorology, 8, 323-334.
- _____ and G. H. Taylor, 1977: Effect of Mountain Terrain on Diffusion in the Planetary Boundary Layer. Joint Conference on Applications on Air Pollution Meteorology, Nov. 29 - Dec. 2, 1977, Salt Lake City, Utah, American Meteorological Society, 119-125.
- Kampé de Fériet, M. J., 1939: Les Fonctions Aléatoires Stationnaires et la Théorie Statistique de la Turbulence Homogène. Ann. Soc. Sci. Brux., 59, 145.
- Littman, F. E., R. W. Griscom and O. Klein, 1976: Regional Air Pollution Study (RAPS). Final Report, Task Order No. 55, Point Source Emission Inventory, Rockwell International, Air Monitoring Center, 1-5.
- Pasquill, F., 1961: The Estimation of the Dispersion of Windborne Material. Meteorological Magazine, 90, 33.
- _____, 1962: Atmospheric Diffusion. D. Van Nostrand Co., Ltd., London, 6-49.
- Rayner, J. N., 1971: An Introduction to Spectral Analysis, Pion, Ltd., London, 75-92.
- Taylor, G. I., 1921: Diffusion by Continuous Movements. Proceedings, London Mathematical Society, Ser. 2, 20, 196.

VITA

Name	Marvin Granville Coleman
Birthdate	November 16, 1949
Birthplace	Washington, D. C.
High School	Pompano Beach Senior High School Pompano Beach, Florida
University	University of South Carolina Columbia, South Carolina 1967-1971 Texas A & M University College Station, Texas 1971-1972 University of Utah Salt Lake City, Utah 1976-1978
Degree	B.S., University of South Carolina Columbia, South Carolina 1971
Honorary Societies	Chi Epsilon Pi
Professional Position	Meteorologist, Captain United States Air Force